



Increased Enrichment for PWRs

Topical Report

ANP-10353NP
Revision 0

January 2021

(c) 2021 Framatome Inc.

Copyright © 2021

**Framatome Inc.
All Rights Reserved**

FRAMATOME TRADEMARKS

ARCADIA, ARTEMIS, ARITA, AREA, GALILEO, COBRA-FLX, S-RELAP5, M5, Q12, GAIA, and HTP are trademarks or registered trademarks of Framatome or its affiliates, in the USA or other countries.

Nature of Changes

Item	Section(s) or Page(s)	Description and Justification
1	All	Initial Issue

Contents

	<u>Page</u>
1.0 INTRODUCTION AND SUMMARY	1-1
2.0 FUEL DESIGNS	2-1
3.0 NEUTRONICS (ARCADIA).....	3-1
3.1 Critical Experiment Comparisons.....	3-1
3.1.1 [].....	3-1
3.1.2 [].....	3-2
3.1.3 [].....	3-3
3.1.4 [].....	3-3
3.1.5 [].....	3-4
3.1.6 Summary of Reactivity Results	3-5
3.1.7 Depletion.....	3-5
3.2 Chromia Doped / Chromium-Coated Cladding Consideration	3-6
3.3 Uncertainty Analysis Disposition.....	3-6
3.3.1 Local Peaking Uncertainty	3-7
3.3.2 Inferred Power Distribution Uncertainty.....	3-9
3.3.3 Calculated Power Distribution Uncertainty	3-10
3.3.4 Detector Sensitivity to Enrichment	3-10
3.3.5 Summary of Uncertainty Analysis Considerations.....	3-12
3.4 Conclusion of Neutronics Disposition.....	3-12
4.0 THERMAL HYDRAULICS	4-1
4.1 CHF Correlation.....	4-1
4.2 COBRA-FLX	4-1
4.3 Fuel Rod Bow	4-2
5.0 MECHANICAL	5-1
5.1 Applicability of Material Methodology.....	5-2
5.2 Applicability of Fuel Rod Thermal-Mechanical Methodology.....	5-4
5.2.1 Temperature Benchmark	5-5
5.2.2 Fission Gas Release, Rod Volume, and Internal Pressure Benchmarks.....	5-5
5.2.3 Radial Power Profiles.....	5-6
5.3 Applicability of Fuel Design Methodology	5-6
5.3.1 Mechanical Performance under Normal Operation and AOO Loads	5-8
5.3.2 Material Changes during Irradiation	5-9

5.3.3	Fuel Rod Thermal-Mechanical Performance.....	5-10
5.3.4	Mechanical Fuel Performance during Postulated Accidents and AOOs.....	5-12
5.4	Applicability of External Loads Methodology.....	5-14
5.5	Applicability of Statistical Hold Down Methodology.....	5-15
5.6	Applicability of Cladding Collapse Methodology	5-16
5.7	Applicability of Fuel Rod Bow Methodology	5-16
6.0	NON-LOCA METHODOLOGY	6-1
6.1	ARITA	6-1
6.1.1	ARCADIA	6-1
6.1.2	S-RELAP5.....	6-4
6.1.3	GALILEO.....	6-4
6.1.4	Key Parameter Review	6-5
6.2	AREA.....	6-6
6.2.1	GALILEO.....	6-6
6.2.2	ARCADIA	6-7
6.2.3	COBRA-FLX.....	6-8
6.2.4	RELAP5	6-9
6.2.5	Key Parameters Review.....	6-10
6.2.6	Criteria	6-10
7.0	LOCA METHODOLOGY	7-1
7.1	SBLOCA	7-2
7.2	RLBLOCA.....	7-2
7.3	LOCA Criteria	7-3
7.4	Conclusions	7-4
8.0	REFERENCES	8-1
	APPENDIX A IMPACT OF ENRICHMENT ON TOPICAL REPORT DECAY HEAT MODELS	A-1

List of Tables

Table 3-1	Reactivity Comparison for Experiments with >5 wt% U-235.....	3-13
Table 3-2	Multi-Assembly Descriptions Using Assemblies Containing >5 wt% U-235.....	3-14
Table 3-3	Multi-Assembly Results	3-15
Table 3-4	Comparison of Multi-Assembly Statistics.....	3-16
Table 5-1	Fuel Centerline Temperature Benchmark Data and Statistics.....	5-18
Table A-1	Topical Reports containing Decay Heat Methods.....	A-13
Table A-2	Comparison of Decay Heat Standards to TRITON results	A-14
Table A-3	Comparison of App K to RLBLOCA Results	A-15

List of Figures

Figure 3-1	Colorset 27 at 0.1 GWd/MTU, Pin Power Relative Percent Difference ..	3-17
Figure 3-2	Colorset 27 at 10 GWd/MTU, Pin Power Relative Percent Difference ...	3-18
Figure 3-3	Colorset 27 at 20 GWd/MTU, Pin Power Relative Percent Difference ...	3-19
Figure 3-4	Colorset 31 at 0.1 GWd/MTU, Pin Power Relative Percent Difference ..	3-20
Figure 3-5	Colorset 31 at 10 GWd/MTU, Pin Power Relative Percent Difference ...	3-21
Figure 3-6	Colorset 31 at 20 GWd/MTU, Pin Power Relative Percent Difference ...	3-22
Figure 3-7	Colorset 33 at 0.1 GWd/MTU, Pin Power Relative Percent Difference ..	3-23
Figure 3-8	Colorset 33 at 10 GWd/MTU, Pin Power Relative Percent Difference ...	3-24
Figure 3-9	Colorset 33 at 20 GWd/MTU, Pin Power Relative Percent Difference ...	3-25
Figure 5-1	Fission Gas Release Logarithmic Predicted/Measured versus Enrichment.....	5-19
Figure 5-2	Rod Volume Logarithmic Predicted/Measured versus Enrichment	5-20
Figure 5-3	Rod Internal Pressure Logarithmic Predicted/Measured versus Enrichment.....	5-21
Figure A-1	Total Decay Heat versus Burnup prior to Shutdown	A-16
Figure A-2	Total Decay Heat versus Enrichment at []	A-17
Figure A-3	Actinide Decay Heat versus Enrichment at []	A-18
Figure A-4	Decay Heat Comparisons, [], All Isotopes	A-19
Figure A-5	Decay Heat Comparisons, [] , Finite Operation, All Isotopes	A-20
Figure A-6	Decay Heat Ratios, []	A-21
Figure A-7	Decay Heat Ratios, []	A-22
Figure A-8	[]	A-23
Figure A-9	[]	A-24
Figure A-10	ARTEMIS versus TRITON Decay Heat at []	A-25
Figure A-11	ARTEMIS versus TRITON Decay Heat at []	A-26
Figure A-12	ARTEMIS versus TRITON Decay Heat at []	A-27

Figure A-13 ARTEMIS versus TRITON Decay Heat at [.....A-28
Figure A-14 ARTEMIS versus TRITON Decay Heat at [.....A-29

Nomenclature

Acronym	Definition
AMS	Aeroball Measurement System
ANS	American Nuclear Society
AOO	Anticipated Operational Occurrence
App K	Appendix K
AREA	ARCADIA Rod Ejection Accident
ARITA	ARCADIA/RELAP Integrated Transient Analysis
ASME	American Society of Mechanical Engineers
BOC	Beginning of Cycle
BOL	Beginning of Life
BU	Burnup
CE	Combustion Engineering
CHF	Critical Heat Flux
CRDM	Control Rod Drive Mechanism
DNB	Departure from Nucleate Boiling
DNBR	Departure from Nucleate Boiling Ratio
ECCS	Emergency Core Cooling System
EM	Evaluation Model
EMDAP	Evaluation Model Development and Assessment Process
EOL	End of Life
FCM	Fuel Centerline Melt
FGR	Fission Gas Release
FRM	Fuel Rod Module
HFP	Hot Full Power
HPU	Hydrogen Pick-up
LAR	License Amendment Request
LHGR	Linear Heat Generation Rate
LOCA	Loss of Coolant Accident
LWR	Light Water Reactor

Acronym	Definition
MEDIAN	Measurement Dependent Interpolation Algorithm using NEM
MLO	Maximum Local Oxidation
NRC	Nuclear Regulatory Commission
NRF	Nuclear Reliability Factor
NUREG	Nuclear Regulatory Guide
OBE	Operating Basis Earthquakes
PCI	Pellet Clad Interaction
PCMI	Pellet Clad Mechanical Interaction
PCT	Peak Cladding Temperature
PIE	Post Irradiation Examination
PIRT	Phenomena Identification and Ranking Table
PWR	Pressurized Water Reactor
RAI	Request for Additional Information
RCS	Reactor Coolant System
REA	Rod Ejection Accident
RIA	Reactivity Insertion Accident
RLBLOCA	Realistic Large Break LOCA
SAFDL	Specified Acceptable Fuel Design Limit
SBLOCA	Small Break LOCA
SPND	Self-Powered Neutron Detector
SRP	Standard Review Plan
SSE	Safe Shutdown Earthquakes
TCS	Transient Clad Strain
THM	Thermal Hydraulic Module
T-H	Thermal Hydraulics
UTL	Upper Tolerance Limit
W	Westinghouse

ABSTRACT

Framatome Inc. (Framatome) has developed a suite of advanced codes and methods for analyzing nuclear power plants. This topical report discusses the codes and methods that support safe operation of the fuel and reactor system. Specifically, this topical report addresses the codes and methods used to perform neutronics analyses, thermal hydraulic analyses, non-LOCA analyses, small break and large break LOCA analyses, and thermal-mechanical fuel evaluations with respect to applicability to fuel with enrichment greater than 5 wt% U-235. Mechanical analysis methodologies used to evaluate the integrity of the fuel assemblies during normal and adverse operations (e.g., external loads, assembly hold down, cladding collapse, and fuel rod bow) are also considered.

Justification for applying the above codes and methods to evaluations of UO₂ fuels with enrichment greater than 5 wt% U-235 as well as analyses of core configurations which include UO₂ fuel with enrichment greater than 5 wt% U-235 is provided in this topical report.

1.0 INTRODUCTION AND SUMMARY

The purpose of this topical report is to justify an increase in the range of applicability for the topical reports which comprise the Framatome advanced codes and methods, as defined by References 1 through 19, to an enrichment limit of [] U-235. The current upper limit is 5 wt% U-235 enrichment.

Fuel assembly designs targeted for implementation for UO₂ fuel with enrichment up to [] U-235 are discussed in Section 2.0.

The following sections provide justification for application of Framatome's codes and methods that will be used for evaluating and analyzing UO₂ fuel with enrichments up to [] U-235:

- Section 3.0: ARCADIA code package (References 1 and 2)
- Section 4.0: Thermal-Hydraulics, including COBRA-FLX (Reference 3) and Critical Heat Flux (CHF) correlations (Reference 4) as well as fuel rod bow (Reference 19)
- Section 5.0: Fuel design and mechanical methodologies (References 12-14, and Reference 17) and Thermal-Mechanical methodologies (References 18 and 19), including material considerations (Reference 15 and 16) and the GALILEO topical report (Reference 11)
- Section 6.0: Non-LOCA Methodology, including ARITA (Reference 5) and AREA (Reference 6)
- Section 7.0: Loss of Coolant Accident (LOCA) Methodology, including Small Break LOCA (SBLOCA, References 7, 8, and 10) and Realistic Large Break (RLBLOCA, References 9 and 10).

2.0 FUEL DESIGNS

Current fuel designs that will be supported by the advanced methods are the GAIA 17x17 design (Reference 14) for Westinghouse (W) plants, the HTP 15x15 design for W plants, and the HTP 14x14 and 16x16 designs for Combustion Engineering (CE) plants. Reference 14 is a modern generic fuel design topical report for the GAIA 17x17 design that was approved by the Nuclear Regulatory Commission (NRC) in 2019. In this context, the word “generic” implies that the design topical report is not applicable to any specific plant. While the design topical report provides a set of criteria which must be satisfied on a plant specific basis, the generic design topical report provides an example of how compliance with the criteria can be satisfied for an example plant. The generic design topical report also describes fuel assembly methods that are primarily comprised of standard mechanical evaluations. There are no modern generic fuel design topical reports for the HTP designs.

Framatome will use the GAIA fuel design topical report to provide the structure (including fuel design criteria) to evaluate the GAIA 17x17 design and the HTP 14x14, 15x15 and 16x16 designs for specific plants. A fuel design evaluation, following the structure of the GAIA topical report, would then be part of the fuel transition license amendment request (LAR) when Framatome fuel is initially loaded into a plant or when fuel with enrichment greater than 5 wt% U-235 is initially loaded.

The criteria and analytical structure described in Reference 14 are not impacted by enrichment.

Other sections in this topical report justify each of the methods (topical reports) that will be used to evaluate the fuel design in accordance with the Reference 14 structure.

3.0 NEUTRONICS (ARCADIA)

3.1 *Critical Experiment Comparisons*

The ARCADIA code package (References 1 and 2) has received NRC approval for use with uranium fuel up to 5 wt% U-235. The comparisons in this section are presented to demonstrate that ARCADIA can accurately model uranium fuel with a U-235 content up to []

The validation provided in References 1 and 2 demonstrated that the models and equations in APOLLO2-A can accurately predict the reactivity of UO_2 fuel. The ability to model fuels with enrichments greater than 5 wt% U-235 is primarily dependent upon the accuracy of the cross section data.

Several critical experiment configurations were selected from the International Handbook of Evaluated Criticality Safety Benchmark Experiments (Reference 21) and evaluated with ARCADIA to demonstrate its adequacy in modeling fuel enrichments up to [] U-235. A summary of the reactivity results (for enrichments from [] U-235) is presented in Section 3.1.6. The results presented justify increasing the range of applicability of ARCADIA up to [] U-235.

3.1.1 []

[] from the Reference 21, Volume 4, [] evaluation were analyzed. []

[]

The benchmark keff values for these experiments varied between []

] with an associated uncertainty of []

The experiments were modeled in APOLLO2-A. Since APOLLO2-A is a 2-dimensional code and []

]

3.1.2 []

[] from the Reference 21, Volume 4, []

] evaluation were analyzed. []

]

The benchmark keff values for these experiments varied between []

] with an associated uncertainty of []

The experiments were modeled in APOLLO2-A. Since APOLLO2-A is a 2-dimensional code and []

]

3.1.3 []

[] from the Reference 21, Volume 4, []

evaluation were analyzed. []

]

The benchmark keff values for these experiments varied between []

[] with associated uncertainties between []

The experiments were modeled in APOLLO2-A. Since APOLLO2-A is a 2-dimensional code and []

]

3.1.4 []

[] from the Reference 21, Volume 4, []

evaluation was analyzed. []

]

This experiment was modeled in APOLLO2-A. Since APOLLO2-A is a 2-dimensional code and [

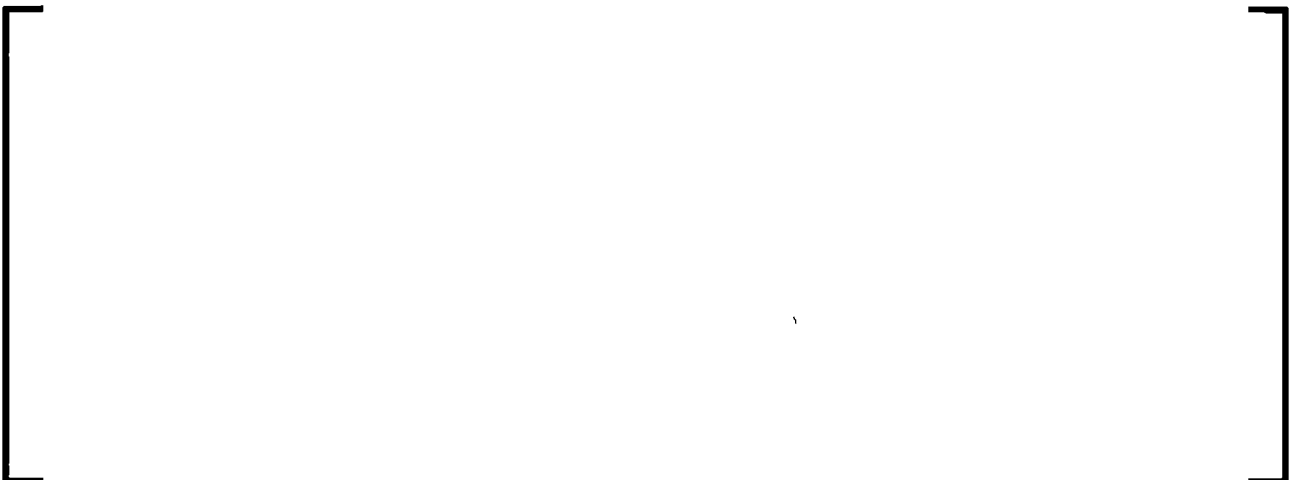
]

3.1.5 []

[] from the Reference 21, Volume 4, []
evaluation was analyzed. [

]

This experiment was modeled in ARTEMIS, using cross sections generated with APOLLO2-A for each of the assembly types. Assemblies in the core were described as follows:



The ARTEMIS calculation was performed using 2x2 radial nodes per assembly.

3.1.6 Summary of Reactivity Results

Reactivity comparisons for each of the experiments described in Section 3.1.1 through Section 3.1.5 are shown in Table 3-1. The calculated-to-measured (C-M) results in this table are expressed in pcm, computed as $(C-M) \times 10^5$.

Differences in reactivity for experiments using fuel rods with greater than 5 wt% U-235 range from [] Reference 2, Section 4.1.1 provide the critical benchmark results for fuel rods with less than or equal to 5 wt% U-235. The differences for the Reference 2 results are between []. The results for the greater than 5 wt% U-235 comparisons are within the range of those accepted in Reference 2.

Based on these results, it is seen that the ARCADIA code system can accurately model configurations with enrichments up to [] U-235.

3.1.7 Depletion

The comparisons to critical experiments given in Section 3.1.6 indicate that APOLLO2-A is accurately calculating the reactivity of fresh fuel assemblies with greater than 5 wt% U-235. Depletion calculations for UO₂ fuel with greater than 5 wt% U-235 use the same equations as for depletion calculations for fuel with less than 5 wt% U-235. The spent fuel analyses and HFP core benchmark calculations presented in Section 4.3 and in Section 5.0 of Reference 2, respectively, show that the equations used for depletion of the fuel provide accurate results for UO₂ fuel. Since these equations are not changing, it is reasonable to conclude that depletion of UO₂ fuel with up to [] U-235 is accurately modeled.

3.2 Chromia Doped / Chromium-Coated Cladding Consideration

Chromia-doped (Cr_2O_3 -doped) UO_2 fuel pellets will be used for enhanced accident tolerant fuel in the future. For these pellets, Chromia is present in the UO_2 fuel region, with the chromium content expected to be on the order of []

Chromium coated cladding will also be used for enhanced accident tolerant fuel in the future. For these fuel rods, a thin layer of Chromium is added to the external surface of an M5 cladding tube. The thickness of the Cr-coating is expected to be on average

[]

Neutronic behavior of a fuel rod is well known and inclusion of chromium as a doping agent or cladding coating does not change the behavior or the ability to calculate reactivity, rod power, or burnup. Addition of chromium reduces the reactivity of a fuel rod due to its absorption characteristics, but these properties are well known and cross sections for chromium isotopes are well established. Inclusion of chromium to the fuel rod, as either a doping agent or a cladding coating, is independent of the U-235 enrichment of the fuel pellet.

3.3 Uncertainty Analysis Disposition

Power distribution uncertainties were developed in Section 8 of Reference 2 for moveable incore fission detectors, fixed Rhodium Self-Powered Neutron Detectors (SPNDs) and Aeroball incore detectors. The ability of ARCADIA to provide predicted and inferred power distributions is dependent upon both local (pin to pin) and global (assembly to assembly) power predictions. The local power component for both types of uncertainties is based on calculated to measured fission rates in critical experiments and on multi-assembly calculations with APOLLO2-A and ARTEMIS.

The uncertainty associated with global power predictions is dependent on comparisons to measured data at commercial nuclear power plants. The global term of the inferred uncertainty is based upon the ability of ARTEMIS to predict power in uninstrumented assemblies using measurements while the global term of the calculation uncertainty is based upon comparisons between predicted and measured values.

3.3.1 Local Peaking Uncertainty

The local peaking uncertainty analysis is composed of two parts: comparisons of predicted and measured pin fission rate results from critical experiments and comparisons of ARTEMIS calculated pin powers to APOLLO2-A calculated results for several multi-assembly configurations (colorsets).

Comparisons of critical experiments determine the accuracy of the APOLLO2-A methodology to calculate the local pin power distribution within a fuel assembly. Fission rate distributions for critical cores using different lattice types were detailed in Section 8.2.1 of Reference 2. Although measured fission rate distributions for critical cores which contain fuel with enrichment greater than 5 wt% U-235 are not available, the conclusions in Section 8.2.1 of Reference 2 are representative of the ability of

[

]
The equations used in determining the pin power distributions are independent of the quantity of the isotopes present. [

1

ARTEMIS to APOLLO2-A comparisons estimate the error of the ARTEMIS dehomogenization with and without burnup compared to an explicit pin model in APOLLO2-A. The local peaking uncertainty analysis in Reference 2 tests the methodology with twenty-four different multi-assembly problems. Additional colorsets using enrichments of [] U-235 were examined to show that the results in Reference 2 are applicable for fuel containing U-235 enrichments up to []. Descriptions for the additional colorsets are given in Table 3-2.

Table 3-3 provides a summary of the results of the local pin powers from each multi-assembly problem, including the colorsets provided in Table 8-4 or Reference 2. All power-producing pins in unrodded assemblies with relative powers greater than [] are considered in the statistical results including Gadolinia pins. The maximum peak to peak relative difference for all the problems is []. The standard deviation of the local pin powers is at or below [] for each of these cases. The mean and standard deviation for the entire set of cases are [] respectively with [].

Pin power relative percent differences are provided for colorsets 27, 31 and 33 at 0.1, 10.0 and 20.0 GWd/MTU in Figure 3-1 through Figure 3-9. In these figures, data is given only for those locations in which the relative power is greater than [].

[] The mean and standard deviation for the peripheral pins are [] respectively with [].

A summary of the statistical analysis is given in Table 3-4. This table shows previous results from Reference 1 and Reference 2 as well as the results when combining data from the Table 3-2 colorsets with those from Reference 2.

Comparing results from the [] as the bounding values, the standard deviation for all colorsets is [] which is [] than the Reference 2 standard deviation value [] but [] than the standard deviation value first introduced in Reference 1 []. This difference [] when combined with the global uncertainty to determine the normal and nonparametric uncertainties would have minimal effects on $F_{\Delta H}$ (or F_R) and F_Q . More importantly, the net effect of this new bounding value will be negligible on the inferred power distribution uncertainty which is less than the typical measurement system uncertainty for $F_{\Delta H}$ (F_R) ([]) and F_Q ([]).

For this reason, the contribution of the ARTEMIS to APOLLO2-A comparisons to the uncertainty analysis in Reference 2 bounds configurations for enrichments up to [] U-235.

3.3.2 Inferred Power Distribution Uncertainty

The portion of the power distribution uncertainty attributed to the ability of ARCADIA to accurately predict power in uninstrumented locations using both measured and predicted values is referred to as the inferred power distribution uncertainty, or global reconstruction uncertainty. Reference 1 provides the description for the INPAX-W and INPAX-CE reconstruction methodologies as well as the MEDIAN Aeroball Measurement System (AMS) reconstruction methodology. Reference 2 extends the MEDIAN reconstruction methodology to Moveable Fission, and Fixed Rhodium detector systems.

For each type of detector system, for each parameter of interest ($F_{\Delta H}$ (F_R for CE plants) or F_Q), a global reconstruction uncertainty is established. For each detector location with measured axial signals, the signals for this detector location are assumed not to exist and the power distribution is reconstructed without this location. The calculated value in the “failed” location is called the “inferred” value. This process is repeated for all detector locations for multiple burnups points, for multiple cycles, and for multiple plants, as available. The database of inferred minus measured values are statistically combined to form the global reconstruction uncertainty. The global reconstruction uncertainty is combined with the local uncertainty components (Section 3.3.1) to estimate the Normal Uncertainty and Non-Parametric Uncertainty, which is then compared to the typical measurement system uncertainty for $F_{\Delta H}$ / F_R or F_Q .

3.3.3 Calculated Power Distribution Uncertainty

The calculated power distribution uncertainty, or Nuclear Reliability Factors (NRFs), are determined using global power prediction and local prediction error terms. A statistical summary of the relative difference between predicted and measured data over the entire database is produced and combined with the local uncertainty components (Section 3.3.1) to estimate the Normal Uncertainty and Non-Parametric Uncertainty calculation uncertainty. Calculation of NRFs is described in detail in Section 8.4 of Reference 2.

3.3.4 Detector Sensitivity to Enrichment

The components of the uncertainty analysis rely on the ability of the codes to predict power distributions and on the comparisons with measured signals during operation. Section 3.3.1 extended the range of calculated local power predictions using colorsets with [] U-235 assemblies. Given measurement results, the methodology for predicting inferred powers in uninstrumented locations and for determining power distributions remains unchanged from Reference 1 and Reference 2 regardless of enrichment. Thus the uncertainty analysis methodology remains applicable to enrichments up to [] U-235.

Currently, there are no commercial U.S. reactors operating with fuel assemblies using enrichments greater than 5 wt%; therefore, power signal measurements are not available for comparisons.

The accuracy of the calculated to measured (or inferred to measured) power comparisons can also be dependent on the incore detector functionality. Functionality of the detectors is not affected by increasing enrichment greater than 5 wt% U-235.

The accuracy of individual detectors is dependent on the following items:

1. Sensitivity, which is not affected by enrichment
2. Background signals
3. Miscellaneous noises (e.g., electronic noise from hardware)
4. Adjustments on measured signals to account for detector aging affects.

Items 2 through 4 are dependent on flux. With higher enriched fuel, the flux is reduced which will increase the importance of background signals and other noise signals and may affect the beta escape probability factor used to define the sensitivity versus material curve for converting the measured signals to account for detector aging.

For moveable incore detectors, the size of the uncertainty on background signals and miscellaneous noise is insignificant. These detectors are insensitive to aging (e.g., detector depletion) effects since they are cross-calibrated to a standard detector.

For fixed incore Rhodium detectors in CE plants, the larger Rhodium signals produced from the large instrument cell decreases the uncertainty of the background signals.

During transition cycles with a wide range of enrichment values, the spread of uncertainty from the correlation for the aging effect on detectors may cause a small, but acceptable, bias in power distributions based on enrichment values.

Differences in the beta escape probability will be seen with higher enriched fuels. This difference will be accounted for during normalization of the power distributions within the monitoring software.

3.3.5 Summary of Uncertainty Analysis Considerations

Because the local and global contributions of the NRFs remain applicable and because the effect on detector operation is small and acceptable with enrichments greater than 5 wt% U-235, the uncertainty analysis documented in Reference 1 (INPAX-W and INPAX-CE) and in Reference 2 (MEDIAN) remains applicable to fuel with enrichments up to [] U-235. Power distributions will continue to be monitored during core operations and comparisons between calculated and measured data will continue to be assessed when data is available.

3.4 *Conclusion of Neutronics Disposition*

Based on the arguments presented in Section 3.1 through Section 3.3, the ARCADIA code system is acceptable for use with fuel enrichments up to [] U-235.

Table 3-1
Reactivity Comparison for Experiments with >5 wt% U-235

Table 3-2
Multi-Assembly Descriptions Using Assemblies Containing >5 wt% U-235

Assembly Type	Number of Assemblies	U-235 Enrichment (wt%)	Other Notes
1	1	5.0	
2	1	5.0	
3	1	5.0	
4	1	5.0	
5	1	5.0	
6	1	5.0	
7	1	5.0	
8	1	5.0	
9	1	5.0	
10	1	5.0	
11	1	5.0	
12	1	5.0	
13	1	5.0	
14	1	5.0	
15	1	5.0	
16	1	5.0	
17	1	5.0	
18	1	5.0	
19	1	5.0	
20	1	5.0	
21	1	5.0	
22	1	5.0	
23	1	5.0	
24	1	5.0	
25	1	5.0	
26	1	5.0	
27	1	5.0	
28	1	5.0	
29	1	5.0	
30	1	5.0	
31	1	5.0	
32	1	5.0	
33	1	5.0	
34	1	5.0	
35	1	5.0	
36	1	5.0	
37	1	5.0	
38	1	5.0	
39	1	5.0	
40	1	5.0	
41	1	5.0	
42	1	5.0	
43	1	5.0	
44	1	5.0	
45	1	5.0	
46	1	5.0	
47	1	5.0	
48	1	5.0	
49	1	5.0	
50	1	5.0	
51	1	5.0	
52	1	5.0	
53	1	5.0	
54	1	5.0	
55	1	5.0	
56	1	5.0	
57	1	5.0	
58	1	5.0	
59	1	5.0	
60	1	5.0	
61	1	5.0	
62	1	5.0	
63	1	5.0	
64	1	5.0	
65	1	5.0	
66	1	5.0	
67	1	5.0	
68	1	5.0	
69	1	5.0	
70	1	5.0	
71	1	5.0	
72	1	5.0	
73	1	5.0	
74	1	5.0	
75	1	5.0	
76	1	5.0	
77	1	5.0	
78	1	5.0	
79	1	5.0	
80	1	5.0	
81	1	5.0	
82	1	5.0	
83	1	5.0	
84	1	5.0	
85	1	5.0	
86	1	5.0	
87	1	5.0	
88	1	5.0	
89	1	5.0	
90	1	5.0	
91	1	5.0	
92	1	5.0	
93	1	5.0	
94	1	5.0	
95	1	5.0	
96	1	5.0	
97	1	5.0	
98	1	5.0	
99	1	5.0	
100	1	5.0	
101	1	5.0	
102	1	5.0	
103	1	5.0	
104	1	5.0	
105	1	5.0	
106	1	5.0	
107	1	5.0	
108	1	5.0	
109	1	5.0	
110	1	5.0	
111	1	5.0	
112	1	5.0	
113	1	5.0	
114	1	5.0	
115	1	5.0	
116	1	5.0	
117	1	5.0	
118	1	5.0	
119	1	5.0	
120	1	5.0	
121	1	5.0	
122	1	5.0	
123	1	5.0	
124	1	5.0	
125	1	5.0	
126	1	5.0	
127	1	5.0	
128	1	5.0	
129	1	5.0	
130	1	5.0	
131	1	5.0	
132	1	5.0	
133	1	5.0	
134	1	5.0	
135	1	5.0	
136	1	5.0	
137	1	5.0	
138	1	5.0	
139	1	5.0	
140	1	5.0	
141	1	5.0	
142	1	5.0	
143	1	5.0	
144	1	5.0	
145	1	5.0	
146	1	5.0	
147	1	5.0	
148	1	5.0	
149	1	5.0	
150	1	5.0	
151	1	5.0	
152	1	5.0	
153	1	5.0	
154	1	5.0	
155	1	5.0	
156	1	5.0	
157	1	5.0	
158	1	5.0	
159	1	5.0	
160	1	5.0	
161	1	5.0	
162	1	5.0	
163	1	5.0	
164	1	5.0	
165	1	5.0	
166	1	5.0	
167	1	5.0	
168	1	5.0	
169	1	5.0	
170	1	5.0	
171	1	5.0	
172	1	5.0	
173	1	5.0	
174	1	5.0	
175	1	5.0	
176	1	5.0	
177	1	5.0	
178	1	5.0	
179	1	5.0	
180	1	5.0	
181	1	5.0	
182	1	5.0	
183	1	5.0	
184	1	5.0	
185	1	5.0	
186	1	5.0	
187	1	5.0	
188	1	5.0	
189	1	5.0	
190	1	5.0	
191	1	5.0	
192	1	5.0	
193	1	5.0	
194	1	5.0	
195	1	5.0	
196	1	5.0	
197	1	5.0	
198	1	5.0	
199	1	5.0	
200	1	5.0	
201	1	5.0	
202	1	5.0	
203	1	5.0	
204	1	5.0	
205	1	5.0	
206	1	5.0	
207	1	5.0	
208	1	5.0	
209	1	5.0	
210	1	5.0	
211	1	5.0	
212	1	5.0	
213	1	5.0	
214	1	5.0	
215	1	5.0	
216	1	5.0	
217	1	5.0	
218	1	5.0	
219	1	5.0	
220	1	5.0	
221	1	5.0	
222	1	5.0	
223	1	5.0	
224	1	5.0	
225	1	5.0	
226	1	5.0	
227	1	5.0	
228	1	5.0	
229	1	5.0	
230	1	5.0	
231	1	5.0	
232	1	5.0	
233	1	5.0	
234	1	5.0	
235	1	5.0	
236	1	5.0	
237	1	5.0	
238	1	5.0	
239	1	5.0	
240	1	5.0	
241	1	5.0	
242	1	5.0	
243	1	5.0	
244	1	5.0	
245	1	5.0	
246	1	5.0	
247	1	5.0	
248	1	5.0	
249	1	5.0	
250	1	5.0	
251	1	5.0	
252	1	5.0	
253	1	5.0	
254	1	5.0	
255	1	5.0	
256	1	5.0	
257	1	5.0	
258	1	5.0	
259	1	5.0	
260	1	5.0	
261	1	5.0	
262	1	5.0	
263	1	5.0	
264	1	5.0	
265	1	5.0	
266	1	5.0	
267	1	5.0	
268	1	5.0	
269	1	5.0	
270	1	5.0	
271	1	5.0	
272	1	5.0	
273	1	5.0	
274	1	5.0	
275	1	5.0	
276	1	5.0	
277	1	5.0	
278	1	5.0	
279	1	5.0	
280	1	5.0	
281	1	5.0	
282	1	5.0	
283	1	5.0	
284	1	5.0	
285	1	5.0	
286	1	5.0	
287	1	5.0	
288	1	5.0	
289	1	5.0	
290	1	5.0	
291	1	5.0	
292	1	5.0	
293	1	5.0	
294	1	5.0	
295	1	5.0	
296	1	5.0	
297	1	5.0	
298	1	5.0	
299	1	5.0	
300	1	5.0	
301	1	5.0	
302	1	5.0	
303	1	5.0	
304	1	5.0	
305	1	5.0	
306	1	5.0	
307	1	5.0	
308	1	5.0	
309	1	5.0	
310	1	5.0	
311	1	5.0	
312	1	5.0	
313	1	5.0	
314	1	5.0	
315	1	5.0	
316	1	5.0	
317	1	5.0	
318	1	5.0	
319	1	5.0	
320	1	5.0	
321	1	5.0	
322	1	5.0	
323	1	5.0	
324	1	5.0	
325	1	5.0	
326	1	5.0	
327	1	5.0	
328	1	5.0	
329	1	5.0	
330	1	5.0	
331	1	5.0	
332	1	5.0	
333	1	5.0	
334	1	5.0	
335	1	5.0	
336	1	5.0	
337	1	5.0	
338	1	5.0	
339	1	5.0	
340	1	5.0	
341	1	5.0	
342	1	5.0	
343	1	5.0	
344	1	5.0	
345	1	5.0	
346	1	5.0	
347	1	5.0	
348	1	5.0	
349	1	5.0	
350	1	5.0	
351	1	5.0	
352	1	5.0	
353	1	5.0	
354	1	5.0	
355	1	5.0	
356	1	5.0	
357	1	5.0	
358	1	5.0	
359	1	5.0	
360	1	5.0	
361	1	5.0	
362	1	5.0	
363	1	5.0	
364	1	5.0	
365	1	5.0	

Table 3-3
Multi-Assembly Results

Set #	Maximum Absolute Relative Difference at BOC (%)	Maximum Absolute Relative Difference Over Entire Depletion (%)	Maximum Absolute Relative Peak to Peak Difference Over Entire Depletion (%)	Standard Deviation of Relative Differences of Each Pin Over Entire Depletion (%)
1				
2				
3				
4				
6				
7				
8				
9				
10				
11				
12				
13				
14				
15				
16				
17				
19				
20				
21				
22				
23				
24				
25				
26				
27				
28				
29				
30				
31				
32				
33				

Table 3-4
Comparison of Multi-Assembly Statistics

	All Colorsets (Colorsets 1-33)	Reference 1 (Colorsets 1-22)	Reference 2 (Colorsets 1-26)
All Pins			
Maximum Peak to Peak Relative			
Standard Deviation of Local Pin Powers (%)			
Number of Data Points			
Mean for All Cases (%)			
Standard Deviation for All Cases (%)			
Peripheral Pins			
Number of Data Points			
Mean for All Cases (%)			
Standard Deviation for All Cases (%)			

Figure 3-1
Colorset 27 at 0.1 GWd/MTU, Pin Power Relative Percent Difference



Figure 3-2
Colorset 27 at 10 GWd/MTU, Pin Power Relative Percent Difference



Figure 3-3
Colorset 27 at 20 GWd/MTU, Pin Power Relative Percent Difference

Figure 3-4
Colorset 31 at 0.1 GWd/MTU, Pin Power Relative Percent Difference



Figure 3-5
Colorset 31 at 10 GWd/MTU, Pin Power Relative Percent Difference



Figure 3-6
Colorset 31 at 20 GWd/MTU, Pin Power Relative Percent Difference



Figure 3-7
Colorset 33 at 0.1 GWd/MTU, Pin Power Relative Percent Difference

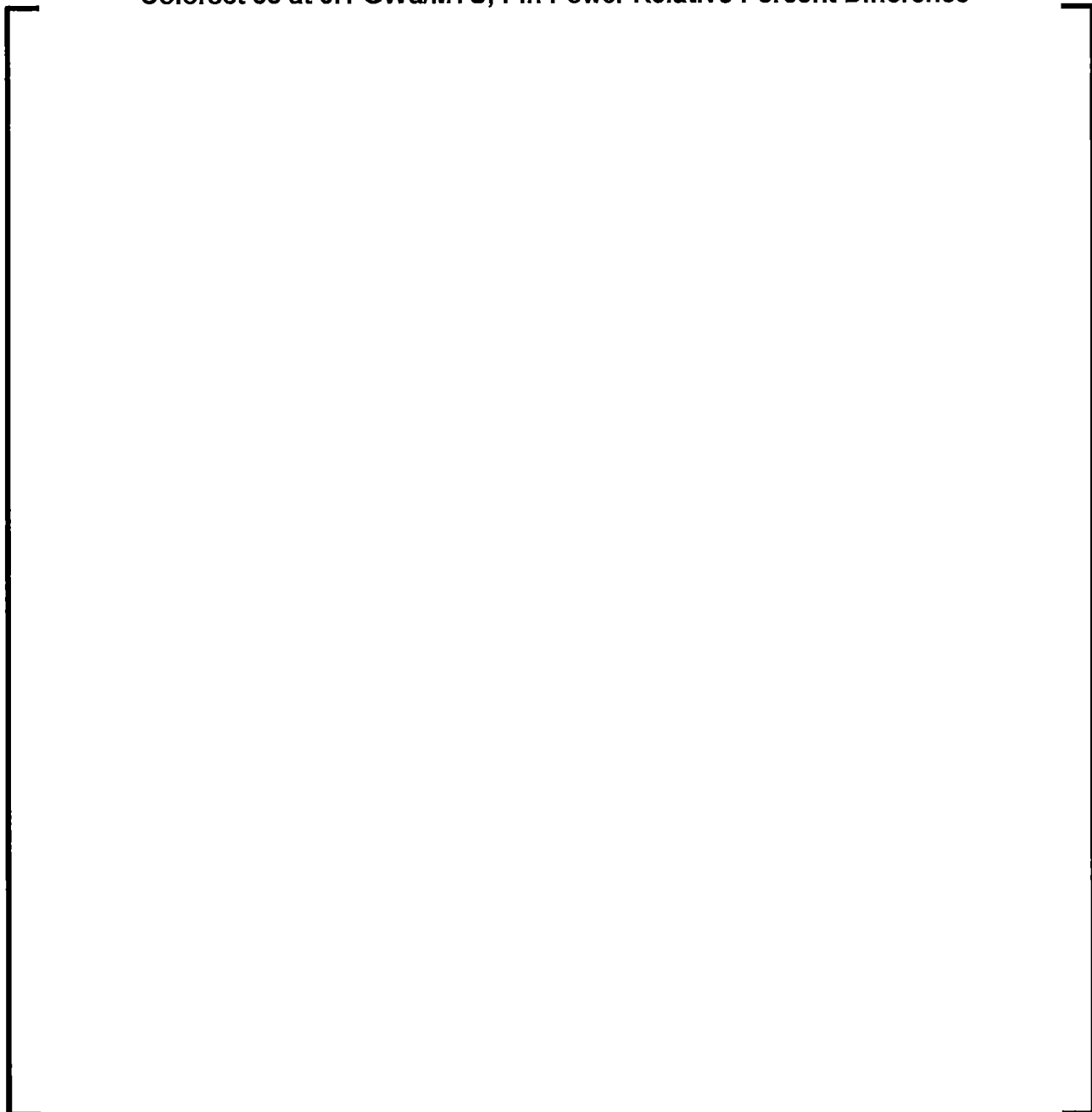


Figure 3-8
Colorset 33 at 10 GWd/MTU, Pin Power Relative Percent Difference

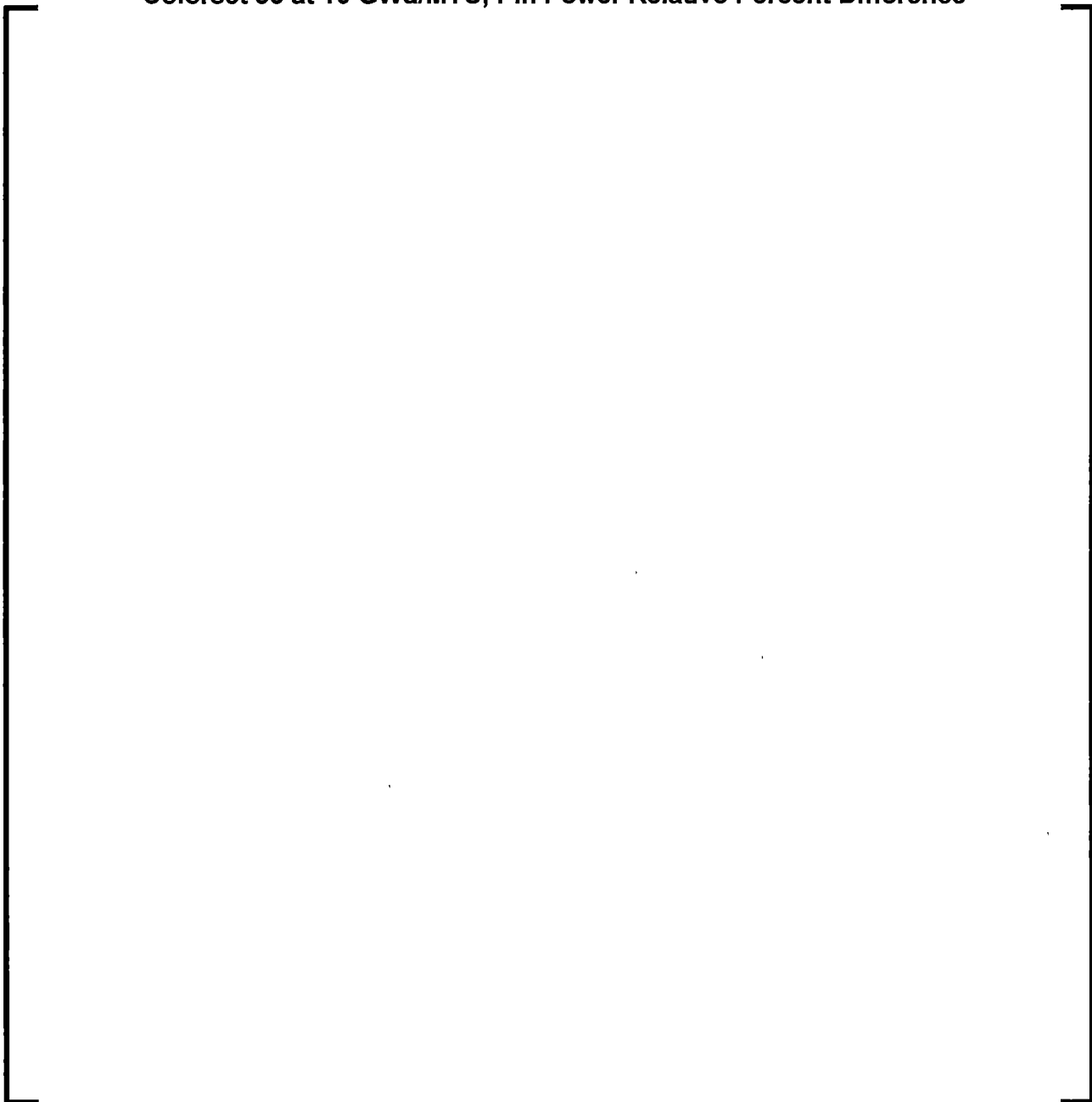
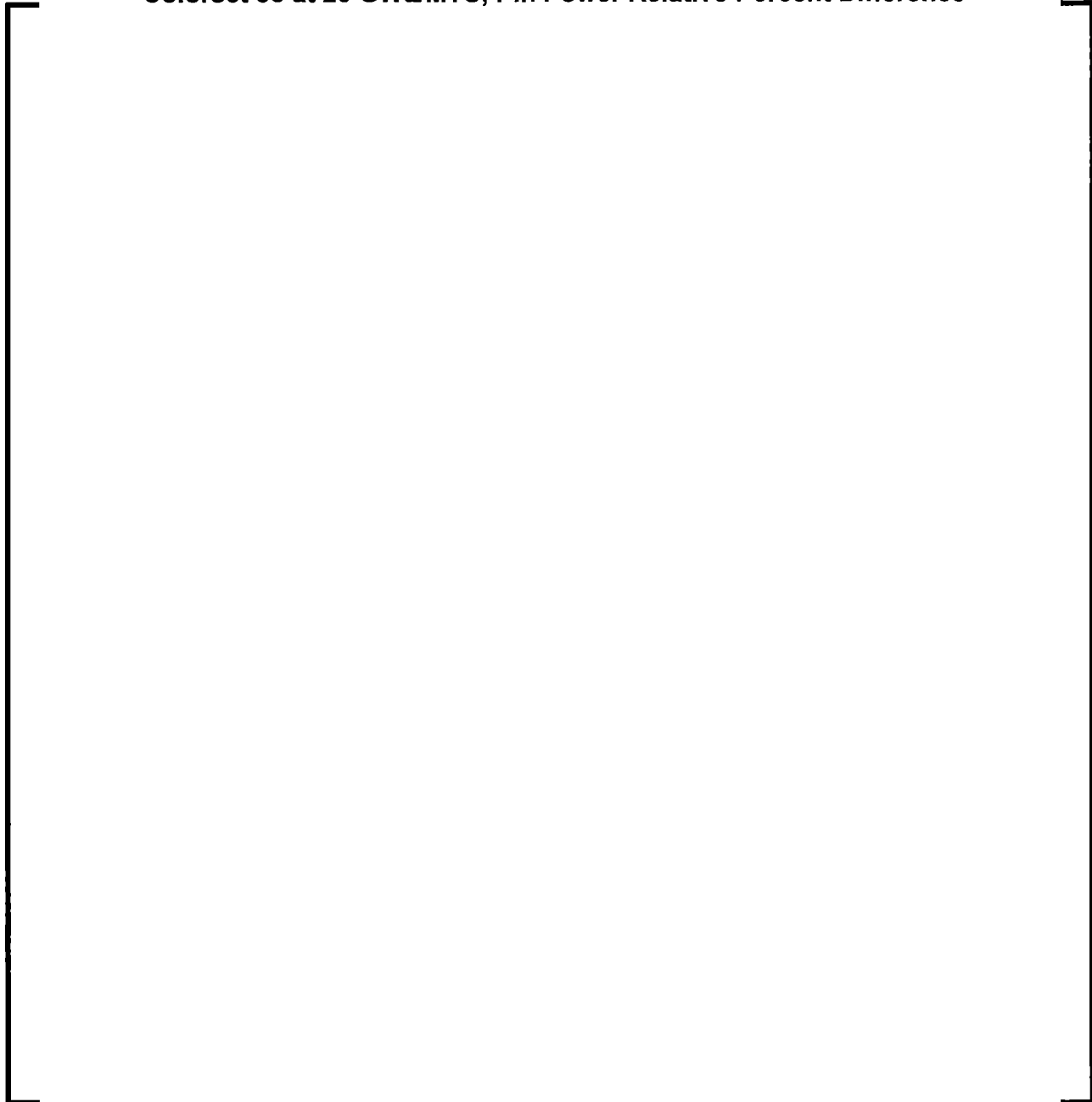


Figure 3-9
Colorset 33 at 20 GWd/MTU, Pin Power Relative Percent Difference



4.0 THERMAL HYDRAULICS

4.1 *CHF Correlation*

CHF is a phenomenon that occurs when a fuel rod is surrounded by a vapor layer which effectively insulates the cladding and the heat transfer coefficient decreases with increasing clad temperature. This state is the Departure from Nucleate Boiling (DNB) condition. Empirical correlations are developed at steady state conditions for each fuel assembly design to determine when this phenomenon may occur. If the heat flux increases beyond this critical condition, a sharp increase in the clad and fuel temperature can occur, which is conservatively assumed to cause cladding failure and, ultimately, fuel rod failure. Since DNB correlations use local conditions—pressure, flow, quality, and heat flux—to predict the onset of DNB and are independent of how those local conditions are generated, such as enrichment, these currently approved CHF correlations are applicable to enrichments greater than 5 wt% U-235.

Appendix C of Reference 3 contains the implementation of the CHF correlations inside COBRA-FLX. These and other NRC approved CHF correlations (such as those found in Reference 4) are also acceptable for use with enrichments greater than 5 wt% U-235.

4.2 *COBRA-FLX*

The COBRA-FLX code (Reference 3) models fluid flow and heat transfer in the reactor core. COBRA-FLX predicts the axial and lateral flow, pressure, and temperature (enthalpy) distributions in rod bundle arrays for flow conditions. Typical applications of the COBRA-FLX code include predictions of core-wide flow and enthalpy distributions as well as pressure drop for steady-state and transient conditions. The code is also used for CHF calculations and Departure from Nucleate Boiling Ratio (DNBR) predictions.

COBRA-FLX possesses a collection of empirical correlations for fluid models and flow properties that allow the computation of pertinent fluid and heat transfer characteristics that are necessary to accurately simulate local flow conditions for operational and safety-related analyses. A review of the empirical correlations approved for use in the COBRA-FLX topical report (Reference 3) supports the conclusion that the correlations are independent of enrichment. The fuel rod model in COBRA-FLX will not be used in safety-related analyses and were excluded from the COBRA-FLX topical review and approval (Reference 3). While the increase in enrichment may impact the input boundary conditions, the increase in enrichment will not impact the ability for COBRA-FLX to accurately model fluid flow and heat transfer in the reactor core. Therefore, the COBRA-FLX topical (Reference 3) will remain applicable for enrichments greater than 5 wt% U-235.

4.3 *Fuel Rod Bow*

Fuel rod bow is the change in the incore gap between fuel rods due to bowing of fuel rods. Reduction of the coolant channel flow area affects the cooling for the fuel rod relative to DNB and reduces local moderation of neutrons, which reduces the local power distribution. Conversely, increasing the coolant channel flow area improves DNB and increases the local power distribution.

Fuel rod bow penalties account for the potential impact on Specified Acceptable Fuel Design Limit (SAFDL) margins due to mechanical distortion resulting from irradiation, effectively changing subchannel flow area and rod-to-rod spacing. Fuel rod bow can increase the local power distribution and decrease the subchannel flow area. These two impacts are accounted for using independent and conservative penalties. The increased local power peaking impacts the Fuel Centerline Melt (FCM) and Transient Clad Strain (TCS) SAFDL evaluation, while the flow area reduction impacts the DNB SAFDL evaluations.

Fuel rod bow is accounted for using the penalties calculated based on the methodology described in Reference 19. Because both DNB and Linear Heat Generation Rate (LHGR) penalties are determined based on parameters not influenced by enrichment, these penalties are acceptable for use with enrichments greater than 5 wt% U-235.

5.0 MECHANICAL

Mechanical fuel design limits are established to meet the relevant requirements of the NRC's regulations consistent with the guidelines outlined in NUREG-0800 Chapter 4.2 (Reference 24). The criteria deal with fuel assembly component performance, with performance determined by the combined response of two or more individual parts (i.e. fuel rod performance, which reflects a complex interaction of cladding, fuel pellet, fill gas, etc.) and material performance. Component performance is analyzed using codes and methods that are defined within NRC approved topical reports. Fuel material performance is part of component performance with advanced materials developed specifically for nuclear applications that also have properties and performance defined within NRC approved topical reports. How these different methodologies are used together to verify compliance to the design criteria through SAFDLs is described within a mechanical design topical report.

Specific mechanical fuel performance methodologies associated with the following topical reports were reviewed to justify applicability for increasing the upper level enrichment limit from 5 wt% to [] U-235.

- M5 (Reference 16) and Q12 (Reference 15) material topical reports (Section 5.1)
- GALILEO fuel rod thermal-mechanical methodology topical report (Reference 11) (Section 5.2)
- Fuel design methodology topical report (Reference 14) (Section 5.3)
- Fuel assembly response to external loads methodology (References 12 and 13) (Section 5.4)
- Fuel assembly statistical hold down methodology (Reference 17) (Section 5.5)
- Fuel rod cladding collapse methodology (Reference 18) (Section 5.6)
- Fuel rod bow methodology (Reference 19) (Section 5.7)

It is demonstrated that increasing enrichment up to [] U-235 (with up to [] Gadolinia) will not affect the methodology or design criteria in the above referenced topical reports.

5.1 *Applicability of Material Methodology*

Fuel material performance is addressed for M5 cladding and spacer grids and Q12 guide tubes and spacer grids. M5 material performance is defined by topical report BAW-10227 (Reference 16). Q12 structural material performance is defined by topical report ANP-10334 (Reference 15). The performance of other fuel assembly materials not associated with a topical report (e.g., nozzles, HMP spacers, end caps) is briefly discussed.

Fuel materials were evaluated to determine whether a change in enrichment would affect material performance. Two keys to the evaluation are (1) the characteristic used to describe fuel exposure and (2) the observation that current experience is sufficient to predict the performance of fuel with higher U-235 enrichment. These are discussed below.

It is important to choose the correct measure of fuel exposure when discussing the effect of irradiation on structural components. Neutron irradiation can cause certain changes, including dimensional changes, increased strength and hardness, and decreased ductility. The mechanism underlying these changes is radiation damage, expressed as the number of displacements per atom. For pressurized water reactors (PWRs), it is common to use fast neutron fluence (energy > 1 MeV) as a surrogate for radiation damage. Because fast fluence is linked more closely than burnup to irradiation effects on structural materials, the evaluation based its discussion of structural parts on fast fluence.

If the U-235 enrichment is increased and the burnup limit is unchanged, the end of life (EOL) fast fluence will be bounded by that for current fuel. A consequence is that current experience is sufficient to understand the effect of increased enrichment on material performance.

The following qualitative argument discusses the distribution of fissions among different types of nuclei, and it uses that distribution to show that the EOL fluence for current enrichment and burnup limits is bounding. (1) Burnup is determined by the density of fissions (number of fissions per unit mass of uranium) and the energy per fission. Most fissions will be from U-235 and Pu-239. The energy release from fission of a U-235 nucleus is similar to that of a Pu-239 nucleus. Therefore, the burnup will be determined almost exclusively by the total density of fissions, and the distribution of fissions among different types of nuclei will not have a significant effect. (2) An increase in U-235 enrichment means that more U-235 nuclei will be available, and therefore the fraction of U-235 fissions will increase, and the fraction of Pu-239 fissions will decrease. (3) The number of fast neutrons released per thermal fission is smaller for U-235 than for Pu-239 (2.42 for U-235 and 2.93 for Pu-239 (Table 1 of Reference 25)). Therefore, the fast fluence at EOL is expected to decrease as the U-235 enrichment increases, and current EOL fluences are bounding.

A similar argument can be made for fast flux. LHGR is determined by the number of fissions per unit of time in a given volume of fuel, and LHGR is limited by thermal-hydraulic considerations, which are independent of enrichment. For a given LHGR and burnup, an increase in U-235 enrichment increases the fraction of U-235 fissions and decreases the local rate of fast neutron production. Therefore, current fluxes are bounding.

The models and properties in the M5 topical report (Reference 16) and the Q12 topical report (Reference 15) were examined and found to depend on various parameters, including time, temperature, burnup, and fast fluence. Some M5 material models, such as those for cladding creep and growth, also depend on fast flux. If the U-235 enrichment is increased and the burnup limit is unchanged, the fast flux and the EOL fast fluence will be bounded by those for current fuel, so current models and properties remain applicable.

Since time and temperature are clearly not affected by enrichment and the current burnup limit is not being changed, increased enrichment is acceptable for the materials in other fuel assembly components such as nozzles, HMP spacers, end caps etc. The discussion above shows that current fluxes and EOL fluences are bounding, so existing analyses remain applicable.

5.2 *Applicability of Fuel Rod Thermal-Mechanical Methodology*

The codes and methods used to analyze fuel rod thermal-mechanical performance are defined within the GALILEO topical report (Reference 11). The predictions of GALILEO rely on a broad set of models that interact in a complex manner to arrive at a final solution of fuel rod performance. Few of these models are direct functions of U-235 enrichment. Radial power profiles are one exception; however, these were determined independently and included in GALILEO as built-in functions.

Rather than perform an exhaustive review of every code model, the overall adequacy of GALILEO for thermal-mechanical fuel rod performance analyses is assessed based on the accuracy of the code predictions of fuel rod centerline temperatures, fission gas release, rod volumes, and rod internal pressures as functions of burnup. These code results are the most important ones for evaluating the thermal-mechanical fuel rod design criteria. The impact of fuel enrichment on these benchmark results are discussed in the next two subsections.

5.2.1 Temperature Benchmark

The extensive GALILEO fuel rod centerline temperature benchmarks are comprised of a total of []

[] The majority of those data points were taken with enrichments between [] U-235. Therefore, the thermal benchmark of GALILEO is well represented in the enrichment range being considered (i.e., up to [] U-235). A summary of the database statistics is shown in Table 5-1, []

[] As seen in the table, the values for 95/95 one-sided upper tolerance limit (UTL) are all approximately equal for data []

[]

Therefore, no negative enrichment bias is observed between these data sets when determining an upper bound centerline temperature.

5.2.2 Fission Gas Release, Rod Volume, and Internal Pressure Benchmarks

The GALILEO Fission Gas Release (FGR), rod volume, and internal pressure benchmark databases are also extensive, consisting of []

[] No unusual trends with enrichment were noted. []

[] This can be seen visually in Figure 5-1, Figure 5-2, and Figure 5-3.

[]

5.2.3 Radial Power Profiles

The method to generate pellet radial power profiles used in the GALILEO fuel rod performance code was reviewed and approved by the NRC in Reference 11. This method is based on the one-dimensional collision-probability depletion code, CIRTHE. The pellet radial power profiles built into GALILEO for LWR fuel cover enrichments up to [] U-235 for UO₂ pellets and up to [] U-235 for Gadolinia pellets.

The same method as approved in Reference 11, using the CIRTHE code, is used to extend the existing radial power profile tables to enrichments up to [] U-235 for Gadolinia pellets with Gadolinia contents up to []

5.3 *Applicability of Fuel Design Methodology*

Fuel system design is performed using analysis methods and codes approved by the NRC to satisfy the guidance in Chapter 4.2 of the Standard Review Plan (SRP, Reference 24). Reference 14 is a modern generic fuel design topical report for the GAIA 17x17 design that was approved by the NRC in 2019. It provides a set of criteria that are generically applicable to fuel designs and which must be satisfied on a plant specific basis. It provides an example of how compliance with the criteria can be satisfied by describing fuel assembly methods that are primarily comprised of standard mechanical evaluations along with specific methodologies defined in other topical reports. The GAIA fuel design topical report provides the structure to evaluate the applicability of the fuel design criteria and methodology to an increase in enrichment up to [] U-235.

Fuel damage criteria and fuel failure criteria as defined within Chapter 4.2 of the SRP are addressed within Sections 5.3.1 through 5.3.4. Fuel rod failure is defined as the loss of fuel rod hermeticity. Fuel rods shall not fail as a result of hydriding, cladding collapse, or overheating of cladding during normal operation including anticipated operational occurrences (AOOs). Failure mechanisms that are more limiting during AOOs and postulated accidents include overheating of fuel pellets, excessive fuel enthalpy, pellet cladding interaction (clad strain and centerline fuel melt), bursting and mechanical fracturing.

The impact of increased enrichment on the analysis of fuel assembly mechanical performance (Section 5.3.1) is addressed as it relates to fuel damage during normal operation including AOOs. Fuel damage criteria assure that fuel system dimensions remain within operational tolerances and that functional capabilities are not reduced below those assumed in the safety analysis.

The impact of increased enrichment on fuel damage criteria and methodology associated with changes to irradiated material properties data are summarized in Section 5.3.2 (e.g., corrosion and dimensional changes).

The impact of increased enrichment on the analysis of fuel rod thermal-mechanical performance is provided in Section 5.3.3. The materials and product forms evaluated are M5 for cladding, UO₂ up to [] U-235, and UO₂-Gd₂O₃ up to [] Gadolinia.

The fuel assembly design must meet the requirements associated with control rod insertability and maintaining a coolable geometry (with adequate coolant channels to permit removal or residual heat) while accounting for severe damage mechanisms and component gross structural deformations related to postulated accidents and severe AOOs described in Chapter 15 of the SRP. The impact of increasing enrichment on the criteria and methodology associated with the mechanical fuel assembly performance during postulated accidents and some AOOs is addressed in Section 5.3.4.

5.3.1 Mechanical Performance under Normal Operation and AOO Loads

Components are subjected to a multitude of loading conditions associated with normal operation, AOOs, shipping and handling activities, and postulated accidents. Stress, strain, and loading limit criteria (SRP Ch. 4.2 Criterion 1.A.i) to prevent fuel damage are based on the mechanical properties of the applicable materials. In the irradiated condition, mechanical properties depend on fast fluence. Since EOL fluences remain bounding with increased enrichment at a given burnup limit, no changes are needed to the models for mechanical properties of fuel cladding and assembly component structural materials. Methods based on conventional open literature equations and general purpose finite element stress analysis codes are not dependent on fuel enrichment. Increased enrichment will not impact the input for the normal operation analysis of assembly components (e.g. Reactor Coolant System (RCS) temperatures, flow, hydraulic lift, hold down loads, and control rod drop impact loads). Conservative input values for fuel rod cladding stress analysis are chosen to bound in-reactor operation and are not affected by the fuel enrichment.

Cyclic loadings which can cause cumulative strain fatigue damage (SRP Ch. 4.2 Criterion 1.A.ii) are not impacted by fuel enrichment. For M5 and Q12 components, the fatigue limits are based on the O'Donnell-Langer model, which does not include a dependence on fast fluence. Other design methods are general methods prescribed in the American Society of Mechanical Engineers (ASME) Code (Reference 26) and are not impacted by fuel enrichment.

Fretting wear can occur at various contact points of the fuel assembly structural members including between fuel assemblies and between control rods and the fuel assemblies (SRP Ch. 4.2 Criterion 1.A.iii). The flow conditions that promote wear are related to the design of the reactor, the fuel assembly mechanical design, and core reload designs. They are not a function of enrichment. Increases in enrichment will not impact the results of fuel rod fretting and wear performance tests.

Unseating of the fuel assembly from the lower core plate guide pins (by allowing lateral displacement) may challenge control rod insertion (SRP Ch. 4.2 Criterion 1.A.vii). The design methodology utilizes conventional open-literature equations to obtain a balance of forces on the fuel assembly in the vertical direction in accordance with previously NRC approved statistical hold down methodologies (References 14, 17, and 27). None of the inputs to the hold down methodology are impacted by increasing the U-235 enrichment since the fluence is expected to be bounded at existing burnups limits (Section 5.5).

Control rod insertability (SRP Ch. 4.2 Criterion 1.A.viii.) can be impacted by fuel assembly structural deformation. An increase in enrichment will not impact stresses and/or load limit criteria as described previously or fuel assembly bow performance, described below.

5.3.2 Material Changes during Irradiation

Corrosion can reduce the material thickness resulting in a lower load carrying capacity and facilitating hydrogen uptake. High rates of hydrogen pick-up (HPU) can impact material ductility. Crud can increase the oxidation rate through increased clad temperature or introducing species (e.g. Lithium) that result in localized accelerated corrosion (SRP Ch. 4.2 Criterion 1.A.iv). Existing models for corrosion and hydriding of M5 (Reference 16) and Q12 (Reference 15), are functions of time at temperature and do not have a dependence on fast flux or fluence. Crud deposition is dependent on coolant chemistry and on heat flux and temperature at the outer surface of the cladding, but it is not related to fuel enrichment. As a result, fuel rod corrosion predictions by GALILEO (Reference 11) will be unaffected by increased enrichment. The use of increased enrichments at current licensed burnup limits [

] will not result in greater oxidation and hydrogen pickup.

Axial and lateral dimensional changes in the fuel rod and fuel assembly can occur due to irradiation growth, irradiation relaxation, creep, thermal expansion, etc. and can cause component to component or component to core interferences (SRP Ch. 4.2 Criterion 1.A.v). This may lead to component failures and/or impacts on thermal hydraulic limits, control rod insertion, and/or handling damage. Enrichment will have no direct impact on empirical fuel rod, fuel assembly, and grid growth models which are functions of burnup (References 15 and 16). Fuel rod bow methods (Reference 19) involve empirical models of fuel rod to fuel rod gap closure as a function of burnup, fuel rod geometry, and assembly span length. These are not impacted by the increasing enrichment at existing burnup limits (Section 5.7). Operating experience and industry feedback are used to establish general design practices (maximize assembly lateral stiffness, minimize guide tube compressive forces, and minimize guide tube creep) intended to minimize fuel assembly bow. Fuel assembly bow performance is monitored through Post Irradiation Examination (PIE) programs to confirm the adequacy of the design with respect to control rod insertability (drop times) and fuel handling. An increase in fuel enrichment will not impact the functionality of these design features since there will be no change in fluence levels impacting the material performance of the fuel assembly components.

5.3.3 Fuel Rod Thermal-Mechanical Performance

Fuel rod thermal-mechanical performance is verified using codes and methodology defined within the GALILEO topical report (Reference 11). The fuel rod internal pressure (SRP Ch. 4.2 Criterion 1.A.vi.) methods during normal operation are defined and the limits are licensed to above system pressure as part of the fuel rod performance code. The impact of enrichments up to [] U-235 on GALILEO code predictions were shown to be acceptable (Section 5.2.2). The cladding collapse (SRP Ch. 4.2 Criterion 1.B.ii.) methodology utilizes the fuel performance code GALILEO to provide initialization data into CROV (Reference 18). The applicability of the CROV methodology is addressed in Section 5.6.

Overheating of cladding (SRP Ch. 4.2 Criterion 1.B.iii.) during normal operation and AOOs leading to fuel rod failure is assumed not to occur if thermal margin criteria (i.e., DNB) are satisfied. DNB criteria are included in CHF correlations associated with a fuel design within the applicable topical reports (References 3 and 4). The impact of increased enrichment on CHF correlations are addressed in Section 4.1.

Fuel rod failure due to the overheating of fuel pellets (SRP Ch. 4.2 Criterion 1.B.iv.) is prevented by FCM criteria. The design criterion is to preclude FCM during normal operation and AOOs. The FCM criterion does not change with increased enrichment. The fuel rod centerline temperature is evaluated using GALILEO in the ARITA methodology (Section 6.1).

Fuel rod failures due to Pellet Clad Interaction (PCI) or Pellet Clad Mechanical Interaction (PCMI) failures (SRP Ch. 4.2 Criterion 1.B.vi.) are prevented. SAFDLs related to Clad Strain and FCM are used to ensure that most PCMI failures are prevented. Clad strain and FCM SAFDLs will not preclude some stress corrosion-assisted failures that occur at low strains or the highly localized overstrain failures introduced by pellet chips on the outer pellet diameter. Manufacturing controls are used to prevent such PCI failures. In addition an increase in U-235 enrichment will result in a more benign environment inside the fuel rods due to decreased iodine inventory. This is due to the fact that increasing U-235 enrichment, for a given burnup, results in a decrease in the number of Pu-239 fissions with an associated increase in U-235 fissions. The cumulative fission yields for iodine isotopes are greater for Pu-239 compared to U-235 which will result in a decreased iodine inventory with an increase in U-235 enrichment.

The absorption of hydrogen by the cladding internally within the fuel rod can lead to local accumulations (hydride lens or platelet) with an associated reduction in material ductility which can lead to failure. The design criteria used to prevent hydriding (SRP Ch. 4.2 Criterion 1.B.i.) are associated with manufacturing controls not related to fuel enrichment (e.g. material limits on the inventory of hydrogen in the fuel pellets and fill gas, fuel rod component cleanliness, and foreign material exclusion).

5.3.4 Mechanical Fuel Performance during Postulated Accidents and AOOs

Enthalpy criteria (SRP Ch. 4.2 Criterion 1.B.v.) and the methods to address the increase in enthalpy due to a Reactivity Initiated Accident (RIA, i.e., control rod ejection) are addressed in Section 6.2.

Clad swelling and rupture criteria (bursting, SRP Ch. 4.2 Criterion 1.B.vii.) and methodology are defined within the evaluation models for SBLOCA and RLBLOCA addressed in Section 7.0. GALILEO methodology is used for the generation of LOCA input.

Mechanical Fracturing (SRP Ch. 4.2 Criterion 1.B.viii.) is a defect in a fuel rod caused by an externally applied force such as a hydraulic load or load derived from core-plate motions (e.g. LOCA or seismic loads). Fuel rod acceptance criteria is associated with protecting against mechanical fracturing via M5 clad stress criteria (Section 5.3.1). Details of the impact of increased enrichment on the criteria and methodology associated with external loads are addressed in Section 5.4.

The criteria and methodology for evaluation of fuel coolability are complex, combining aspects of materials performance, fuel component performance, and performance of other systems such as the emergency core cooling system (ECCS). In addition to structural stability that is addressed via preclusion of fuel rod mechanical fracturing, clad melting and embrittlement are also addressed. These later two use input from GALILEO and other codes and methods that are discussed in the applicable LOCA methodology sections (see Section 7.0).

Current cladding embrittlement criteria (SRP Ch. 4.2 Criterion 1.C.i.) from 10 CFR 50.46 (b) is associated with peak clad temperature, maximum cladding oxidation, and maximum hydrogen generation. The oxidation performance of fuel cladding and the rate of hydrogen generation are independent of fuel enrichment.

In severe RIAs, such as rod ejection, the large and rapid deposition of energy in the fuel can result in melting, fragmentation, and dispersal of fuel (SRP Ch. 4.2 Criterion 1.C.ii.). The mechanical action associated with fuel dispersal can be sufficient to destroy the cladding and impact the rod-bundle geometry. The impact of increasing enrichment on control rod ejection methodology is addressed in Section 6.2.

Generalized (i.e., non-local) melting of the cladding could result in the loss of rod-bundle fuel geometry (SRP Ch. 4.2 Criterion 1.C.iii.). Criteria associated with cladding embrittlement are considered more stringent than generalized melting criteria for M5 cladding.

To meet ECCS performance requirements during accidents, the analysis of the core flow distribution must account for clad burst strain and flow blockage caused by ballooning (swelling) of the cladding (SRP Ch. 4.2 Criterion 1.C.iv.). Clad swelling and rupture criteria and methodology are defined within the evaluation models for SBLOCA and RLBLOCA (Section 7.0). Cladding properties for the models were determined from tests in the EDGAR facility on cladding without fuel, so there is not a dependence on enrichment. GALILEO methodology is used for generation of LOCA inputs.

Earthquakes (Operating Basis Earthquakes (OBE) and Safe Shutdown Earthquakes (SSE)) and postulated RCS pipe breaks during LOCA result in external forces on the fuel assembly. The fuel assembly is designed to withstand these loads without loss of the capability to perform the safety functions that are commensurate with these events (Structural deformation, SRP Ch. 4.2 Criterion 1.C.v. – Appendix A). Methodology, which is independent of U-235 enrichment, has been developed to address the dynamic response of the fuel assembly to external seismic or LOCA loads (Section 5.4).

5.4 *Applicability of External Loads Methodology*

Earthquakes (OBE and SSE) and postulated RCS pipe break (LOCA) stresses and/or load limit criteria are in accordance with NRC approved topical report ANP-10337 (Reference 12, including supplement 1, (Reference 13)). Limits are defined according to the ASME code (Reference 26) and SRP Chapter 4.2, Appendix A, unless otherwise specified. Spacer grids, guide tubes, and fuel rods are subject to more stringent service limits due to their specific special functions (i.e., ensuring coolable geometry is maintained, forming a path for control rod insertion, and protecting the fission product barrier). An increase in enrichment does not change the cladding and structural material behavior since EOL fluence values will not increase at existing burnup limits.

The acceptance criterion for spacer grids in OBE conditions corresponds to a small amount of plastic deformation without buckling and is established through grid impact load limit testing. The acceptance criteria for SSE/LOCA performance of the spacer grids are also established through grid impact load limit testing. Spacer grid deformation is not to exceed a permanent deformation limit which has been shown to maintain a path for control rod insertion and does not challenge coolability of the fuel assembly. [

] These criteria are based on testing. [] are accounted for through an approved simulated-EOL testing protocol. These loads limits will not be impacted by an increase in enrichment because current EOL fluences are bounding at existing burnup limits.

Sudden and severe changes in the geometry of the guide tubes shall not occur (e.g., local collapse or plastic hinging). Stresses are not to exceed a limit prohibiting local collapse and assuring that there is critical buckling load margin. These criteria are established at beginning of life (BOL) and EOL. These loads limits will not be impacted by an increase in enrichment because current EOL fluences are bounding at existing burnups limits.

Numerical models simulate the mechanical behavior of fuel assemblies in the vertical and horizontal directions. These models capture the motion of the fuel due to the external excitation and the interaction between neighboring fuel assemblies and the core baffle as applicable. The results of the analyses are used to calculate impact loads and stresses, which are compared to the allowable values for each structural component. Methodology involving material properties and loads from seismic and LOCA events is not dependent on fuel enrichment.

5.5 *Applicability of Statistical Hold Down Methodology*

Unseating of the fuel assembly from the lower core plate guide pins (by allowing lateral displacement) may challenge control rod insertion.

Design criteria state that the hold down springs shall maintain fuel assembly contact with the lower support plate (without lift-off) during normal operation conditions and AOOs (with the exception of a pump over-speed transient). During a pump over-speed transient, the assembly may lift-off as long as both the top and lower nozzles maintain engagement with the core alignment pins and the hold down springs maintain positive hold down margin after the event.

The design methodology utilizes conventional open-literature equations to obtain a balance of forces on the fuel assembly in the vertical direction in accordance with the NRC approved topical reports ANP-10342 (Reference 14) and BAW-10240 (Reference 27), including the statistical hold down methodology described within topical report BAW-10243 (Reference 17). The forces are due to fluid friction loss, buoyancy, momentum change, hold down spring force, and gravity. The evaluation includes the assessment of bounding operating conditions (including coolant temperatures and flow rates, mixed and homogeneous cores, BOL and EOL conditions), component dimensional characteristics (including reactor core plate to core plate distance, fuel assembly lengths, plus hold down spring deflections and mechanical set), and material characteristics (including thermal expansion, irradiation growth and relaxation, and spring rate). The guide tube growth model from the applicable NRC approved topical

report is used to determine the fuel assembly growth bounds. Uncertainties are accounted for by using a combination of deterministic and statistical methods.

None of the inputs to the hold down methodology are impacted by increasing the U-235 enrichment since the fluence is bounding at existing burnup limits.

5.6 *Applicability of Cladding Collapse Methodology*

If axial gaps in the fuel column result from pellet densification, initial as-fabricated axial gaps, or axial gap creation during shipping and handling, the cladding has the potential to collapse into the gap. The clad will ovalize and flatten due to the strains and fail. The criterion for cladding collapse is that the predicted creep collapse life of the fuel rod must exceed the maximum expected in-core life.

Fuel rod creep collapse methodology is described in Reference 18.

The cladding collapse methodology utilizes the fuel performance code GALILEO (Reference 11) to provide initialization data into CROV (Reference 18) for M5 clad fuel rods (Reference 16). Within GALILEO, code models are demonstrated to be acceptable [] (Section 5.2). []

As stated in Section 5.1, fast fluences are lower at higher enrichments at the same burnup. Therefore, the models with fast flux dependence, such as clad creep, remain applicable and the code predictions are acceptable.

5.7 *Applicability of Fuel Rod Bow Methodology*

Axial and lateral dimensional changes in the fuel rod can occur due to irradiation growth, irradiation relaxation, creep, thermal expansion, etc. These may lead to impacts on thermal hydraulic limits.

Fuel rod bow methods involve empirical models of fuel gap closure versus burnup.

Material properties such as growth, relaxation, creep, and thermal expansion are a function of fluence, which is bounding at existing burnups limits. Therefore the applicability of the empirical models and criteria are not impacted by increased enrichment.

Fuel Rod Bow Methods involve DNBR and LHGR burnup thresholds for which penalties are applied as described within Reference 19. [

] The impact of an increase in enrichment on the methodologies for determining fuel rod bow DNBR and LHGR penalties are addressed in Section 4.2.

Table 5-1
Fuel Centerline Temperature Benchmark Data and Statistics



Figure 5-1
Fission Gas Release Logarithmic Predicted/Measured versus
Enrichment

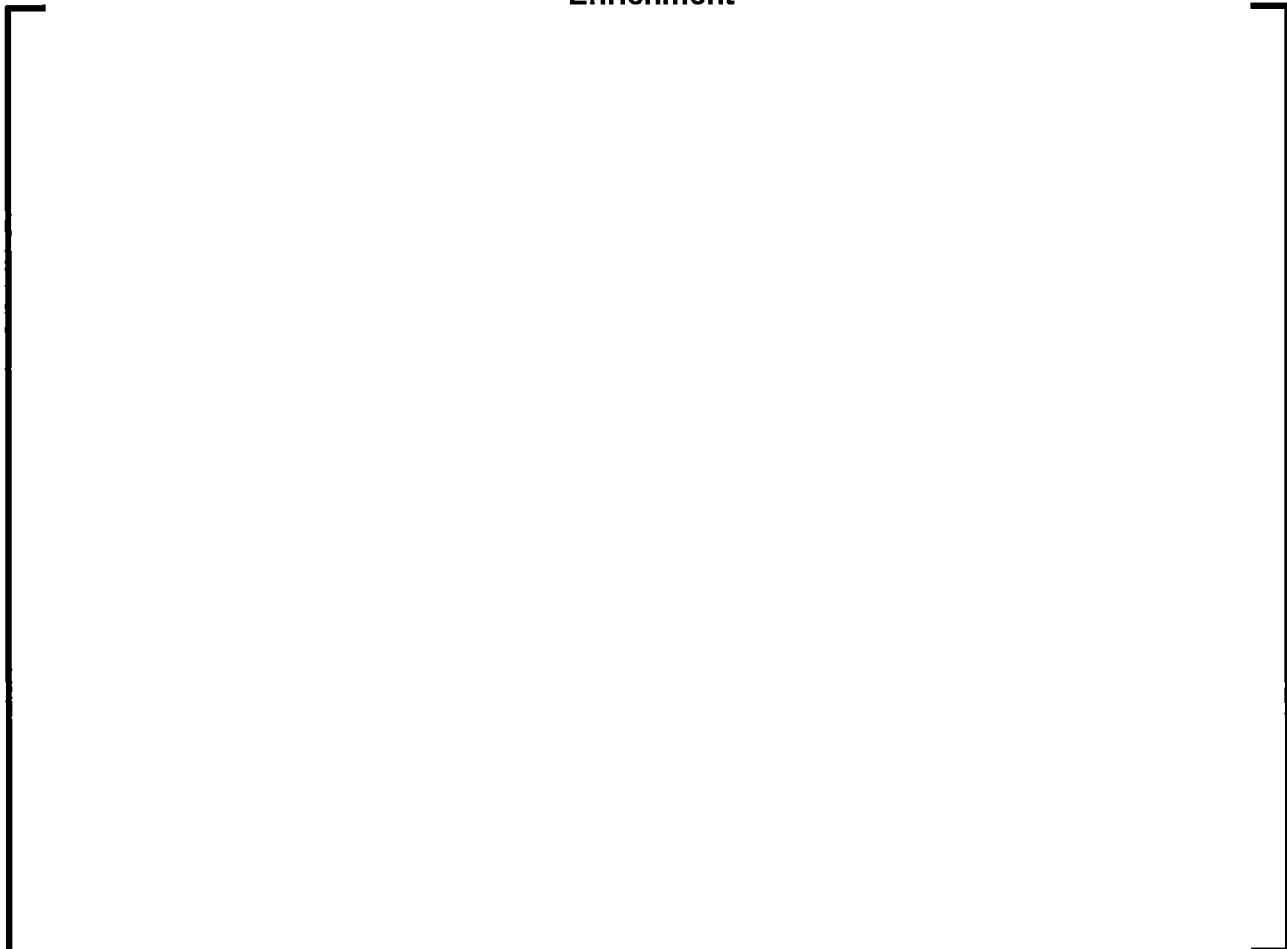


Figure 5-2
Rod Volume Logarithmic Predicted/Measured versus Enrichment

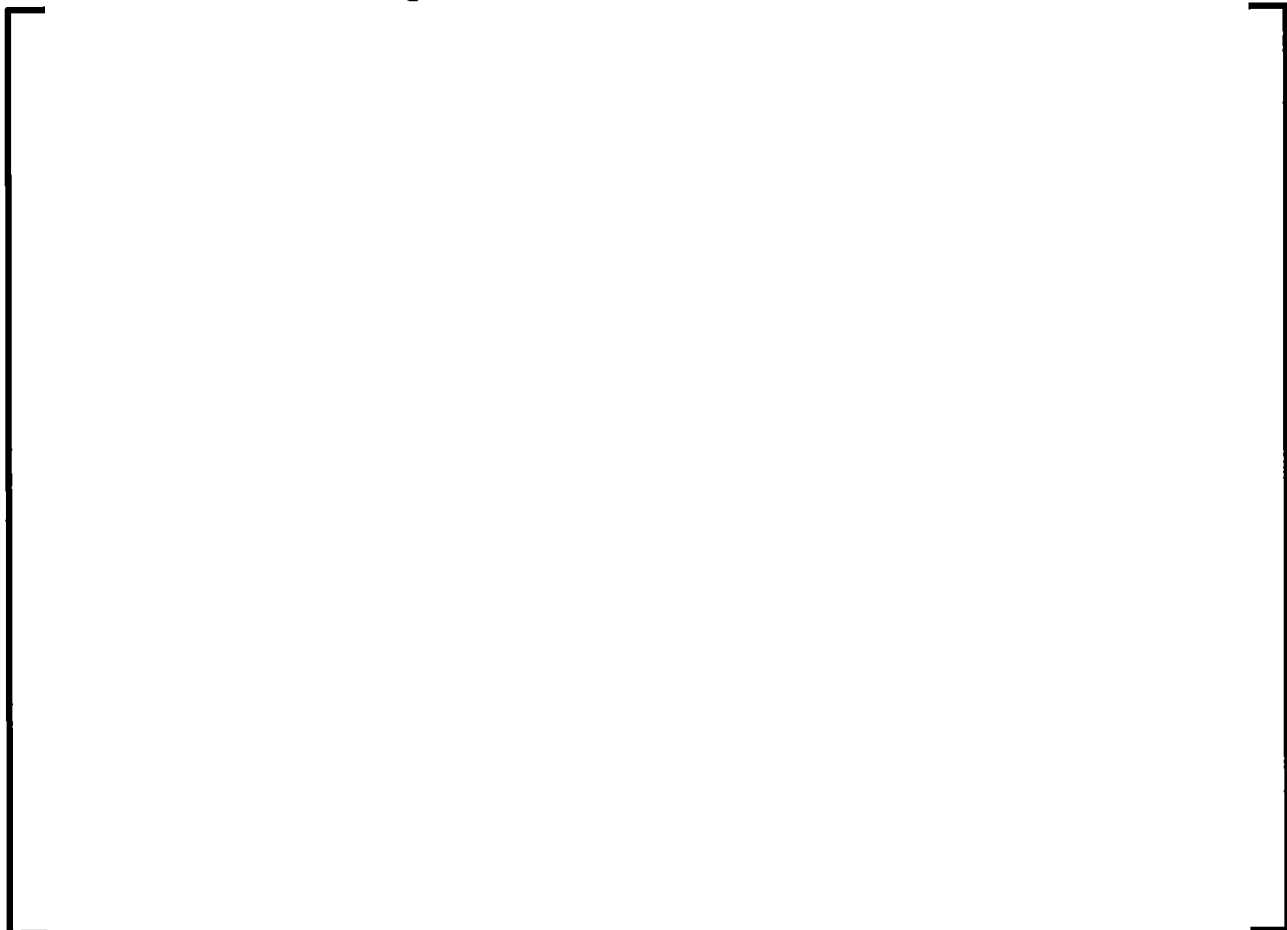
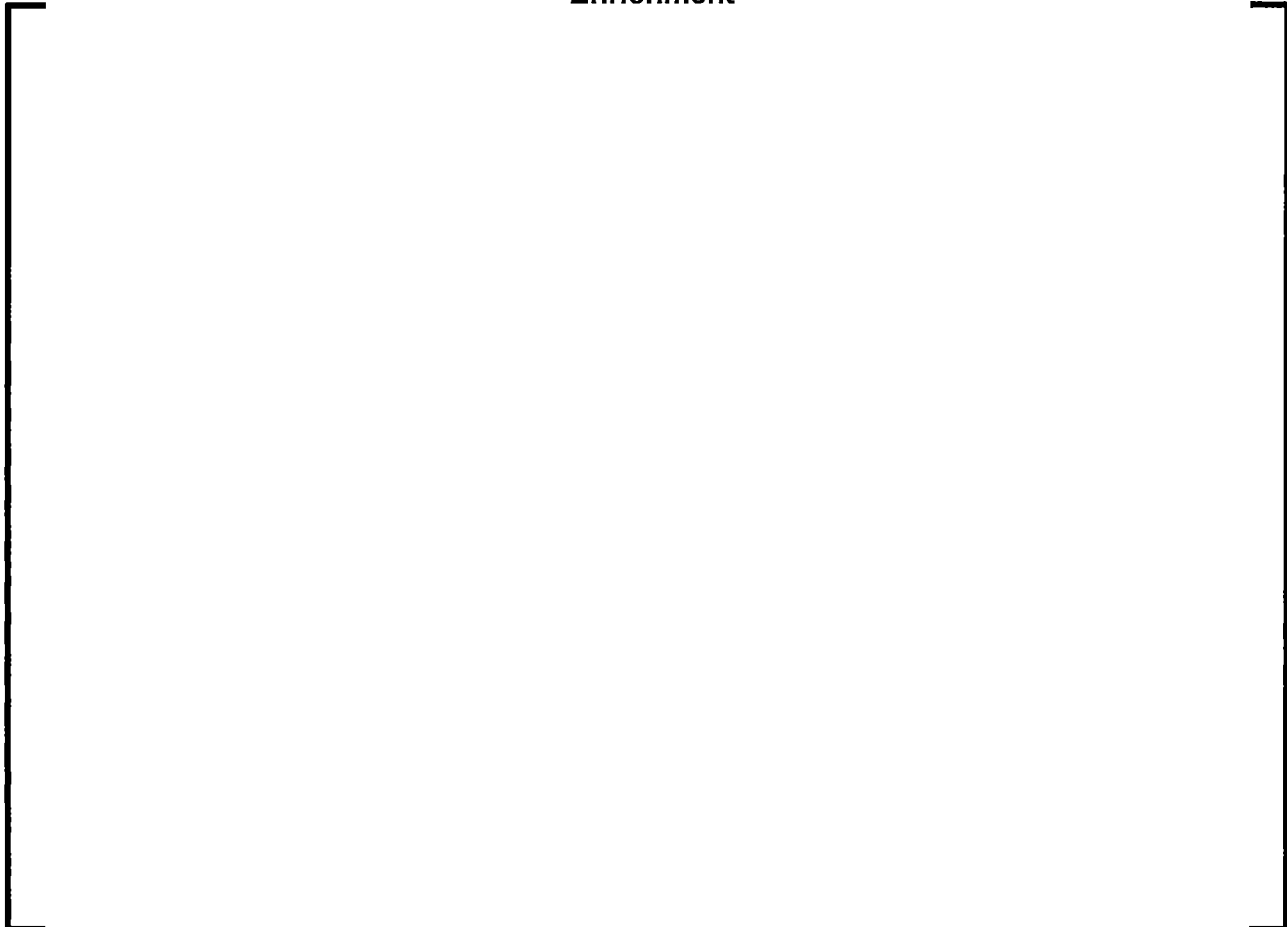


Figure 5-3
Rod Internal Pressure Logarithmic Predicted/Measured versus
Enrichment



6.0 NON-LOCA METHODOLOGY

6.1 ARITA

Reference 5 presents the ARCADIA/RELAP Integrated Transient Analysis (ARITA) methodology for evaluation of Non-LOCA transients with the exception of the control rod accident in a PWR. The ARITA methodology provides a realistic, plus uncertainties, representation of the reactor response during Non-LOCA transients and demonstrates compliance with the appropriate criteria.

The ARITA Non-LOCA methodology relies on three primary codes: (ARCADIA, (Reference 2), GALILEO (Reference 11), and S-RELAP5. ARTEMIS is composed of a neutronics portion (Reference 2) and a thermal hydraulic portion (Reference 3).

6.1.1 ARCADIA

6.1.1.1 APOLLO2-A

Several benchmarks of APOLLO2-A to critical experiments are described in Section 3.1.1 through Section 3.1.4. The fuel enrichment in these experiments is

【] U-235.

Reactivity differences from comparisons to the referenced experiments are within the observed differences presented in Section 4.1.1 of Reference 2. These results demonstrate that the cross section data from the APOLLO2-A library provides a correct representation of fuel with a U-235 enrichment greater than 5 wt%. No fission rate experiments for U-235 enrichments greater than 5 wt% are available, but with the results from the critical experiments, it is expected that APOLLO2-A will continue to provide an accurate representation of assembly pin power distributions for enrichment up to 【] U-235.

A series of multi-assembly calculations were evaluated using APOLLO2-A and ARTEMIS. The purpose of these calculations is to compare the dehomogenized ARTEMIS pin power distributions against the APOLLO2-A pin power distributions. Several configurations with enrichments greater than 5 wt% U-235 were examined as discussed in Section 3.3.1. This is the same process described in Section 8.2.2 of Reference 2. Results of the multi-assembly analysis show that the statistics are comparable with those presented in Section 12.2.2 of Reference 1 and Section 8.2.2 of Reference 2. Based on these comparisons the ARTEMIS dehomogenization process remains valid for fuel assemblies with uranium enrichments greater than 5 wt% U-235.

6.1.1.2 ARTEMIS

Justification for the use of ARTEMIS in the ARITA methodology is provided in Section 8.3 of Reference 5. Since an increase in enrichment does not require changes to either the APOLLO2-A or ARTEMIS codes, the behavior of the codes remains the same and all comparisons and justifications made in Reference 5 remain valid. Justification for ARCADIA with enrichment greater than 5 wt% U-235 for use with ARITA is based on the information presented in Section 3.0.

6.1.1.2.1 Decay Heat

ARTEMIS uses the ANSI/ANS-5.1 2005 Decay Heat standard (Reference 23). Justification of APOLLO2-A and ARTEMIS codes to this standard for application with enrichments greater than 5 wt% U-235 are provided in Appendix A.

6.1.1.2.2 ARTEMIS THM

COBRA-FLX is the ARTEMIS Thermal-Hydraulics Module (THM). Enrichment has no impact on the results from the THM. The THM calculations are dependent on heat flux, flow, and water properties in the assembly. Since the comparisons of the multi-assembly analysis show that ARTEMIS is capable of accurately producing pin powers, then the heat flux to the THM is also correct. Flow and water properties are not impacted by enrichment. The justifications provided in Sections 8.4 of Reference 5 remain valid for use of the THM in ARTEMIS.

6.1.1.2.3 ARTEMIS FRM

The ARTEMIS Fuel Rod Module (FRM) is described in Section 5.0 of Reference 1. The validation for this model was performed through comparisons to a fuel performance code as described in Section 5.0 of Reference 1. Additional comparisons were made to GALILEO in Section 5.2.2 of the Reference 6 topical report. These comparisons include several radial power distributions for both annular and solid fuel pellets. The similarities between the ARTEMIS FRM and GALILEO are addressed in the response to RAI 2 of Reference 6. The calculation of thermal fuel rod behavior has been proven for the ARTEMIS FRM through comparisons to GALILEO and from results of plant data. As stated in Section 6 of Reference 20, GALILEO is acceptable for enrichments up to [] U-235. Likewise, based on similarities and comparisons between ARTEMIS and GALILEO, the ARTEMIS FRM is applicable for application with fuel enrichments up to [] U-235.

6.1.1.2.4 ARTEMIS System Analysis

The [] was evaluated using ARTEMIS (see Section 3.1.5). This core has fuel with enrichments greater than 5 wt% U-235. Using the standard 2x2 core nodal model in ARTEMIS, the difference in the comparison was []. This case along with the critical experiment comparisons provide evidence that as a complete system, ARTEMIS using data generated by APOLLO2-A is capable of analyzing reactor cores with enrichments up to [] U-235.

6.1.2 S-RELAP5

The ARITA methodology (Reference 5), Section 8.2.1, examines the general S-RELAP5 modeling of phenomena and processes important to the analysis of Non-LOCA events. The phenomena and processes are addressed in more detail in ANP-10339Q1P (Reference 20), but the general high level perspective is sufficient for the review to determine if there is any impact from an increase in enrichment. The phenomena and processes listed in Reference 5, Section 8.2.1 are:

Primary Coolant System

1. Reactor Vessel Mixing
2. Pressurizer Phenomena
3. Flashing of Coolant in the Reactor Vessel Upper Head
4. Choking/Critical Flow

Secondary Coolant System

1. Primary/Secondary Heat Transfer
2. Flashing of MFW Downstream of Isolation Valve
3. Choking/Critical Flow
4. Flashing of Tube Rupture Effluent
5. Boiler Region Mixture Level

A review of these phenomena and processes indicates that none of these are a function of or impacted by enrichment.

6.1.3 GALILEO

GALILEO is the best-estimate fuel performance code which models the thermal and mechanical behavior of individual PWR fuel rods during normal operation and transient conditions. GALILEO is used to calculate FCM and TCS for the ARITA methodology, using post-processed data from the ARTEMIS/S-RELAP5 execution.

The impact of increasing enrichment on the GALILEO models was provided in Section 5.0. Enrichment, as an input to GALILEO, is used only to provide an appropriate radial power profile. Radial power profile tables are included in GALILEO for enrichments up to [] U-235. GALILEO was shown to be acceptable for use with enrichments up to [] U-235 (Section 5.2).

The use of GALILEO with respect to the ARITA methodology remains applicable for enrichments up to [] U-235.

6.1.4 Key Parameter Review

In addition to the codes used in the ARITA methodology, key neutronics parameters were checked to determine if any impact due to increased enrichment exists. The parameters directly addressed by the ARITA methodology are listed in Table 2.1 of Reference 20:

- Neutronics: rod worth, delayed neutron fraction, Doppler reactivity feedback, moderator reactivity feedback, rate of reactivity insertion, neutron velocities, reactor trip reactivity, and excore flux.
- Thermal (Neutronic and Detailed Model): fuel conductivity, gap conductance, clad conductivity, heat capacity of fuel and clad, direct energy deposition in coolant, pellet radial power profile, RCS pressure, RCS temperature, RCS flow, and peaking.

An increase in the U-235 enrichment above 5 wt% will not have an impact on these parameters. As discussed previously, the behavior of APOLLO2-A and ARTEMIS with enrichments greater than 5 wt% U-235 are consistent with what has been observed for application with enrichments less than 5 wt% U-235. Therefore, the behavior of the codes in generating the key neutronics parameters for ARITA is not changed and generation of these key parameters will continue to be within the same range of uncertainty as previously stated.

6.2 AREA

Reference 6 presents the ARCADIA Rod Ejection Accident (AREA) methodology for evaluation of a control rod accident in a PWR. The AREA methodology provides a conservative representation of the reactor response during an REA and demonstrates compliance with the appropriate criteria. The methodology makes use of a variety of codes and methods. The ARCADIA code system (References 1 and 2) is used to analyze the three dimensional neutronics and thermal-hydraulics behavior during the transient. The GALILEO code (Reference 11) provides the thermal-mechanical properties of the fuel pins. The RELAP5 code is used to model the reactor coolant system response.

The AREA methodology was designed to be consistent with the regulatory guidance for a control rod ejection accident (see Reference 22). The methodology is flexible and capable of demonstrating compliance with potential revisions to the Rod Ejection Accident (REA) criteria, including various formulations of criteria related to enthalpy, DNBR, fuel temperature, fuel pin pressure, transient FGR, and RCS pressure. These criteria are included in the methodology as various forms of input and can be modified as necessary to incorporate future changes to the criteria as specified by the NRC.

The analytical models for the AREA methodology include GALILEO, ARTEMIS, COBRA-FLX, and RELAP5 models. The impact of increasing U-235 enrichment on each of these models is discussed below.

6.2.1 GALILEO

GALILEO is the fuel performance code that provides the following information pertinent to the AREA methodology:

- Enthalpy rise criteria functionalized by clad corrosion is converted to enthalpy rise limits versus burnup. The clad corrosion model for oxide thickness or hydrogen uptake is used to maximize the corrosion obtained at a given burnup to obtain an enthalpy rise limit with burnup.

- Fuel thermal properties with burnup dependencies for the time dependent solutions of temperature. These include heat capacity for the fuel pellet and clad, radial power distribution in the fuel pellet, porosity of the fuel, and gap conductance.
- Fuel pin internal pressure to determine fuel enthalpy limits for high clad temperature failure criteria.

The impact of increasing enrichment on the GALILEO models was provided in Section 5.0. Enrichment, as an input to GALILEO, is used only to provide an appropriate radial power profile. Radial power profile tables are included in GALILEO for enrichments up to [] U-235. GALILEO was shown to be acceptable for use with enrichments up to [] U-235 (Section 5.2). GALILEO predictions for fuel pin internal pressure were shown to be acceptable in Section 5.2.2. Section 5.3.2 concludes that corrosion prediction by GALILEO will be unaffected by increased enrichment.

The use of GALILEO with respect to the AREA methodology remains applicable for enrichments up to [] U-235.

6.2.2 ARCADIA

The ARCADIA code system is a neutronics, fuel thermal, and thermal-hydraulic code that performs core design and safety evaluations. It has 3-D neutronics static and transient solvers with time dependent fuel and coolant models. It is used as the core transient model for AREA.

The ability of ARCADIA to model cores with enrichments up to [] U-235 was discussed in Section 3.1 and Section 3.3.1. Section 3.1 presented comparisons with critical experiments. Reactivity differences seen for these experiments were similar to the differences seen for experiments presented in Reference 2, Section 4.1.1. These results demonstrate that the cross section data is a correct representation of fuel with U-235 content greater than 5 wt%.

As part of the AREA methodology, the dehomogenization method in ARTEMIS is used to calculate a []

U-235 was validated through the comparison of multi-assembly calculations presented in Section 3.3.1.

The use of ARCADIA with respect to the AREA methodology remains applicable for enrichments up to [] U-235.

6.2.2.1 Gap Conductance and Thermal Conductivity Models

Section 5.2.2 of Reference 6 discusses comparisons between GALILEO and the ARTEMIS fuel thermal model to verify use of the gap conductance tables. These comparisons include several radial power distributions for both annular and solid fuel pellets. Additional information for GALILEO with respect to the ARTEMIS FRM - GALILEO comparisons is addressed in the response to RAI 2 of Reference 6. Based on these comparisons, it was concluded in Reference 6 that the temperature of the fuel pellet and clad are well captured by ARTEMIS.

As stated in Section 5.2, GALILEO is acceptable for use with enrichments up to [] U-235. Based on similarities and comparisons between ARTEMIS and GALILEO, the ARTEMIS FRM is applicable for application with fuel enrichments up to [] U-235.

6.2.3 COBRA-FLX

COBRA-FLX is the THM used in the core simulator ARTEMIS and is used for both the nodal simulator and the detailed [] Validation of COBRA-FLX is found in Reference 3.

The THM calculations are mainly dependent on heat flux, flow and water properties within the assembly. The ability to calculate heat flux is directly related to the ability to calculate pin powers. The multi-assembly analysis in Section 3.3.1 demonstrated the ability of ARTEMIS to accurately produce pin power distributions for enrichments up to [] U-235.

Flow and water properties are not impacted by enrichment.

Applicability of COBRA-FLX and the CHF correlations implemented inside COBRA-FLX are discussed in Sections 4.1 and 4.2 and were found to be acceptable for use with enrichments greater than 5 wt% U-235.

Based on the above discussion, use of COBRA-FLX within ARCADIA with respect to the AREA methodology remains applicable for enrichments up to [] U-235.

6.2.4 RELAP5

The purpose of the RELAP5 computer code for AREA is twofold: 1) to calculate the pressure response during an REA, taking no credit for the possible pressure reduction caused by the assumed failure of the Control Rod Drive Mechanism (CRDM) pressure housing, and 2) to provide a pressure boundary condition to the core transient model for the DNBR calculation, if required. The RELAP5 computer code models the primary and secondary systems that determine the change in RCS pressure, inlet temperature, and/or flow during an REA simulation.

The calculations performed by RELAP5 during an AREA analysis are not affected by enrichment. Any enrichment effect would be caused by the input neutronic parameters. Specifically, the power and heat flux shapes are generated by ARTEMIS and passed to RELAP5, either by coupled interfaces or manual input. The ARTEMIS calculations, as discussed in Section 6.2.2, are applicable for enrichments up to [] U-235.

Based on the above discussion, the use of RELAP5 within the AREA methodology is applicable for enrichments up to [] U-235.

6.2.5 Key Parameters Review

In addition to the codes used in the AREA methodology, key parameters were checked to determine if these would be impacted by increased enrichment. The parameters directly addressed by the AREA methodology are listed in Table 4-3 of Reference 6:

- Neutronics: ejected rod worth, delayed neutron fraction, moderator feedback, fuel temperature feedback, rate of reactivity insertion, neutron velocities, reactor trip reactivity, ejected rod location, and excore flux.
- Thermal (Neutronic and Detailed Model): fuel conductivity, gap conductance, clad conductivity, heat capacity of fuel and clad, direct energy deposition in coolant, pellet radial power profile, RCS pressure, RCS temperature, RCS flow, and peaking.

The above parameters are not impacted by increasing the U-235 enrichment of the fuel. For calculated values, the acceptability of the codes used for AREA was determined in the previous sections. The non-calculated values (rate of reactivity insertion, control rod location) are input to the analysis and are not dependent on enrichment.

6.2.6 Criteria

As previously stated, NRC criteria for REAs is provided in Reference 22 and include allowable limits for fuel rod cladding failure thresholds (Reference 22, Section 3) and peak radial average fuel enthalpy for core coolability (Reference 22, Section 6). Peak radial average fuel enthalpy for high-temperature cladding failure thresholds is provided as a function of cladding pressure differential and is based on overheating of the pin. For PCMI, peak radial average fuel enthalpy rise is a function of excess hydrogen and is based on the thermal stress of the pellet on the clad. The limit for peak radial average fuel enthalpy for core coolability is a restriction of the energy deposited to prevent significant changes to the fuel geometry from severe thermal effects. U-235 enrichment

does not affect the thermal, mechanical, or chemical properties of the pellet. Therefore, none of these thresholds is dependent on U-235 enrichment.

Appendix B of Reference 22 provides guidance on the calculation of transient fission gas release, which was shown to be sensitive to fuel burnup and peak radial average fuel enthalpy rise. For burnups below and above 50 GWd/MTU, transient fission gas release is shown as a function of peak radial average fuel enthalpy regardless of enrichment. Conclusion of FGR being independent of enrichment is supported by the GALILEO disposition discussed in Section 5.2.2. Thus, the guidance for calculation of transient fission gas release can be applied to enrichment up to [] U-235 with use of the appropriate peak radial average fuel enthalpy rise value.

Hydrogen uptake models are discussed in Appendix C of Reference 22 and are found to be dependent on cladding type. Cladding type is not a function of enrichment. Thus, the hydrogen uptake models provided in the Reference 22 guidance is applicable to UO₂ fuel with enrichments up to [] U-235.

7.0 LOCA METHODOLOGY

The SBLOCA methodology is defined in References 7, 8, and 10, while the RLBLOCA methodology is defined in References 9 and 10. This section justifies increasing the range of applicability for Reference 7 through Reference 10 to [] U-235 enrichment.

The scope of the evaluation of an increase in enrichment on the Framatome LOCA evaluation models (EMs) focuses on the direct effects that a change in enrichment would have on the methods, which include topical reports and the models and correlation embedded in the referenced LOCA analysis codes. Framatome's SBLOCA EM is defined in EMF-2328P-A (Reference 7) and EMF-2328 Supplement 1P-A (Reference 8). Framatome's RLBLOCA EM is defined in EMF-2103P-A Revision 3 (Reference 9). The GALILEO fuel performance code is implemented in both the SBLOCA and RLBLOCA EMs via ANP-10349P (Reference 10).

The SBLOCA and RLBLOCA methodologies rely on two computer codes; GALILEO (Reference 11) and S-RELAP5. The impact of increasing enrichment up to [] U-235 on GALILEO is addressed in Section 5.2. The impact of an increase in enrichment up to [] U-235 on the decay heat models used in both SBLOCA and RLBLOCA is addressed in Appendix A. This section focuses on the impact an increase in enrichment up to [] U-235 on the LOCA EMs separate from the issues addressed for GALILEO in Section 5.2 and for the decay heat models in Appendix A.

7.1 SBLOCA

The SBLOCA EM was reviewed with respect to an increase in enrichment up to

[] U-235. []

The evaluation also identified the important fuel-related SBLOCA phenomena that could potentially be affected by increased enrichment. []

[] The impact on the decay heat

model is addressed in Appendix A. The review of the models simulating the remaining phenomena found that the modeling in the current SBLOCA EM remains valid for fuel with enrichments greater than 5 wt% U-235.

[]

7.2 RLBLOCA

The RLBLOCA EM was developed using the Evaluation Model Development and Assessment Process (EMDAP). Therefore, a graded EMDAP approach was used to evaluate the impact of the increased enrichment to the RLBLOCA EM. []

[] The RLBLOCA Phenomena Identification and Ranking Table (PIRT) defined in Table 5-1 of

Reference 9 was used to identify phenomena and modeling that may be impacted by increased enrichment. The PIRT review identified the following fuel-related RLBLOCA models that could potentially be affected by the increased enrichment: [

] The impact on the decay heat model is addressed in Appendix A. The review of the remaining models found that the modeling in the current RLBLOCA EM remains valid for fuel with enrichments greater than 5 wt% U-235.

[

] The effect of increased enrichment on GALILEO is discussed in Section 5.2.

7.3 ***LOCA Criteria***

10 CFR 50.46 provides the U.S. NRC acceptance criteria for ECCS for light-water nuclear power reactors. Analyses are performed with NRC-approved evaluation models to demonstrate that calculated ECCS cooling performance following postulated LOCA's conforms to the criteria set forth in paragraph (b) of 50.46. Briefly, 10 CFR 50.46 limits the calculated results such that:

1. The Peak Cladding Temperature (PCT) is less than 2200 °F
2. The total Maximum Local Oxidation (MLO) is less than 17 percent of the total cladding thickness
3. The maximum hydrogen generation is less than 1% of the hypothetical amount that would be generated if all of the metal in the cladding cylinders reacted
4. The core geometry remains amenable to cooling
5. Long-term core cooling is maintained

The current regulation, including the criteria specified above, is explicitly applicable to “uranium oxide pellets within cylindrical Zircaloy or ZIRLO cladding”. Increased enrichment only alters the abundance of various isotopes of uranium in the fuel pellet. Therefore, fuel pellets with increased enrichment remain “uranium oxide pellets” compositionally. Thus, the LOCA criteria set forth in paragraph (b) of 10 CFR 50.46 remain applicable to fuel with enrichments greater than 5 wt% U-235.

7.4 *Conclusions*

Framatome's SBLOCA and RLBLOCA EMs as supplemented by GALILEO were evaluated for an increase in enrichment up to [] U-235. The LOCA EMs (References 7, 8, 9, and 10) and their constitutive models and correlations potentially impacted by the enrichment change were reviewed. Several items, []

[] (Section 7.1)

and the decay heat models (Appendix A) implemented in both the SBLOCA and RLBLOCA EMs, were identified as potentially impacted. []

[]

Both decay heat models used by the LOCA EMs are validated for increased enrichment fuel in Appendix A. Based on the findings and evaluations performed, it is concluded that the Framatome SBLOCA and RLBLOCA EMs with GALILEO implemented are valid and acceptable for licensing applications for enrichments up to [] U-235.

8.0 REFERENCES

1. ANP-10297P-A, Revision 0, "The ARCADIA® Reactor Analysis System for PWRs Methodology Description and Benchmarking Results," February 2013.
2. ANP-10297P-A, Revision 0, Supplement 1P-A, Revision 0, "The ARCADIA® Reactor Analysis System for PWRs Methodology Description and Benchmarking Results," August 2018.
3. ANP-10311P-A, Revision 1, "COBRA-FLX: A Core Thermal-Hydraulic Analysis Code," October 2017.
4. ANP-10341P-A, Revision 0, "The ORFEO-GAIA and ORFEO-NMGRID Critical Heat Flux Correlations," September 2018.
5. ANP-10339P, Revision 0, "ARITA - ARTEMIS/RELAP Integrated Transient Analysis Methodology," August 2018.
6. ANP-10388P-A, Revision 0, "AREA™ – ARCADIA® Rod Ejection Accident," December 2017.
7. EMF-2328(P)(A), Revision 0, "PWR Small Break LOCA Evaluation Model, S-RELAP5 Based," March 2001.
8. EMF-2328(P)(A), Revision 0, Supplement 1(P)(A), Revision 0, "PWR Small Break LOCA Evaluation Model, S-RELAP5 Based," December 2016.
9. EMF-2103P-A, Revision 3, "Realistic Large Break LOCA Methodology for Pressurized Water Reactors," June 2016.
10. ANP-10349P, Revision 0, "GALILEO Implementation in LOCA Methods," October 2020.
11. ANP-10323P-A, Revision 1 "GALILEO Fuel Rod Thermal-Mechanical Methodology for Pressurized Water Reactors," November 2020.
12. ANP-10337P-A, Revision 0, "PWR Fuel Assembly Structural Response to Externally Applied Dynamic Excitations," April 2018.

13. ANP-10337, Revision 0, Supplement 1P-A, Revision 0 "Deformable Spacer Grid Element," September 2018.
14. ANP-10342P-A, Revision 0, "GAIA Fuel Assembly Mechanical Design," September 2019.
15. ANP-10334P-A, Revision 0, "Q12TM Structural Material," September 2017.
16. BAW-10227P, Revision 2, "Evaluation of Advanced Cladding and Structural Material (M5) in PWR Reactor Fuel," December 2019.
17. BAW-10243P-A, Revision 0, "Statistical Fuel Assembly Hold Down Methodology," September 2005.
18. BAW-10084P-A, Revision 3 "Program to Determine In-Reactor Performance of BWFC Fuel Cladding Creep Collapse," July 1995.
19. XN-75-32(P)(A), Supplements 1-4, "Computational Procedure for Evaluating Fuel Rod Bowing," February 1983.
20. ANP-10339Q1P, Revision 0, "Response to Request for Supplemental Information – ANP-10339P," March 2019.
21. International Handbook of Evaluated Criticality Safety Benchmark Experiments, Nuclear Energy Agency, July 2018 (NEA/NSC/DOC(95)03).
22. "Pressurized-Water Reactor Control Rod Ejection and Boiling-Water Reactor Control Rod Drop Accidents," Regulatory Guide RG 1.236, US NRC, June 2020.
23. ANSI/ANS-5.1-2005 American National Standard for Decay Heat Power in Light Water Reactors, American National Standards Institute, Inc., April 1, 2005.
24. NUREG-0800, Standard Review Plan, Section 4.2, "Fuel System Design", Rev. 3, March 2007.
25. DOE-HDBK-1019/2-93, DOE Fundamentals Handbook: Nuclear Physics and Reactor Theory, Volume 2, January 1993.
26. American Society of Mechanical Engineers Boiler and pressure Vessel Code, Section III, Nuclear Power Plant Components, 1992 Edition.

27. BAW-10240(P)-A, Revision 0, Incorporation of M5TM Properties in Framatome ANP Approved Methods, May 2004.

28. SCALE 6.2.3 Reference: B.T. Reardon and M.A. Jessee, Eds., "SCALE Code System," ORNL/TM-2005/39, Version 6.2.3, Oak Ridge National Laboratory, Oak Ridge, Tennessee, 2018.

29. ANSI/ANS-5.1-1979 American National Standard for Decay Heat Power in Light Water Reactors, American National Standards Institute, Inc., August 29, 1979.

30. ANSI/ANS-5.1-2014 American National Standard for Decay Heat Power in Light Water Reactors, American National Standards Institute, Inc., November 4, 2014.

31. ANSI/ANS-5.1-1971 Proposed ANS Standard for Decay Energy Release Rates Following Shutdown of Uranium-Fueled Thermal Reactors, American Nuclear Society, October 1971.

APPENDIX A
IMPACT OF ENRICHMENT ON TOPICAL REPORT DECAY HEAT
MODELS

Decay heat is characterized by the buildup of fission products and actinides during power production and subsequent decay during shutdown. Decay heat is an important phenomenon in evaluation of the consequences for some chapter 15 events. This appendix addresses the impact of increasing enrichment up to [] U-235 with respect to the decay heat models used in Framatome methodologies.

The currently approved, or in review, Topical Reports that incorporate decay heat models are listed in Table A-1 with a short description and references. The current range of applicability of these topical reports is as follows:

- Enrichment: \leq 5 wt% U-235
- Pin Burnup: up to 62 GWd/MTU
- No limitation on power density
- Range of applicability based on the NRC approved topical reports, not necessarily the decay heat standards that the topical reports are based on.

TRITON (Reference 28) is used to provide a best estimate decay heat model as a base reference condition. For each topical report decay heat model, an evaluation of the fission product and actinide decay heat is provided versus enrichment and demonstrates that the model remains conservative relative to the best estimate model.

A.1 *TRITON Calculations with ORIGEN*

The best estimate effects of decay heat with U-235 enrichment as calculated by the SCALE Package (Reference 28) are used as a basis to evaluate decay heat models employed by Framatome. The SCALE code system is a widely-used modeling and simulation suite for nuclear analysis that has been verified and validated for criticality safety, reactor and lattice physics, radiation shielding, spent fuel and radioactive source term characterization and sensitivity and uncertainty analysis. TRITON is a multipurpose SCALE control module used for reactor physics and is coupled with ORIGEN to obtain depletion effects in reactor cores. The TRITON module that is used in the analysis is the 2-D multi-group transport solution module (NEWT). The SCALE 6.2.3 code utilizes ENDF/B-VII.1 nuclear data libraries for continuous energy and multi-group neutronics. ORIGEN tracks 174 actinides, 1149 fission products and 974 activation products. Decay data include all ground and metastable state nuclides with half-lives greater than 1 millisecond. The nuclide tracking in ORIGEN is based on the principle of explicitly modeling all available nuclides and transitions in the current fundamental nuclear data for decay and neutron-induced transmutations, relying on cross section and decay data in ENDF/B VII. Cross section data for materials and reactions not available in ENDF/B-VII are obtained from the JEFF-3.0/A special purpose European activation library containing 774 materials and 23 reaction channels with 12,617 neutron-induced reactions below 20 MeV.

SCALE 6.2.3 is used as a best estimate reference to compare to the Framatome decay heat models to show applicability to enrichments up to [] U-235.

The GAIA fuel assembly (Reference 14) which is a 17x17 lattice is used for the reference decay heat calculations. Depletions are performed at rated power for

[]

Figure A-1 presents the amount of total decay heat at full power operation prior to shutdown as a function of burnup for different enrichments.

Observations made from this figure are:

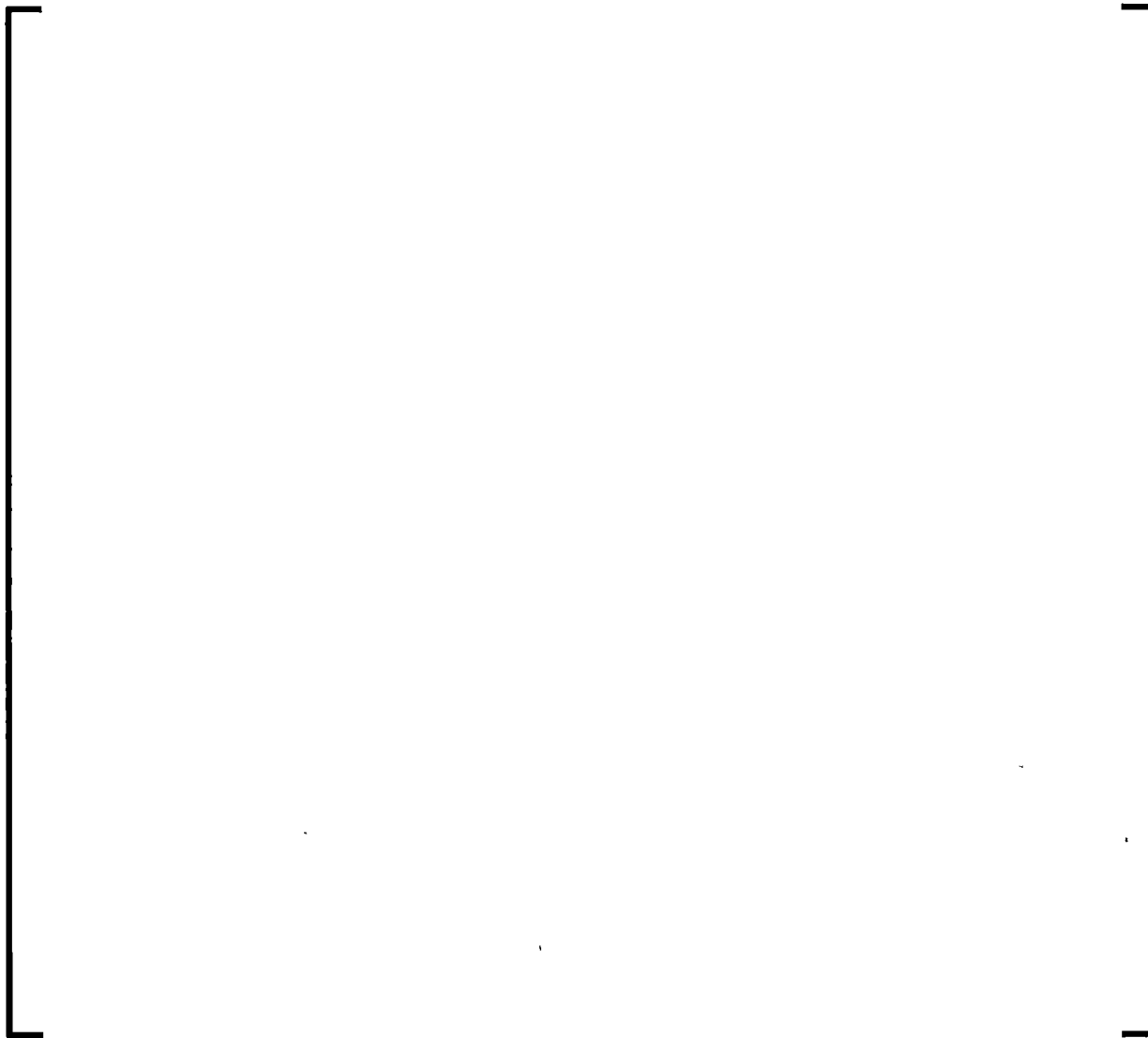


Figure A-2 shows the variation of total decay heat with enrichment at [] for several shutdown times, in seconds. The behavior is [] with enrichment. Since the enrichment behavior is [] U-235 are evaluated in the remaining sections to demonstrate that the decay heat models are valid for fuel with enrichments up to [] U-235.

Figure A-3 presents the actinide decay heat at [] versus enrichment for different shutdown times. The behavior is []

]

The results from these simulations are used in the evaluation of the decay heat models discussed in subsequent sections.

A.2 RLBLOCA Decay Heat Model

The decay heat model for RLBLOCA (Reference 9) uses []

]

A.2.1 RLBLOCA Fission Product Decay Heat

Section 8.5.1.17 of Reference 9 demonstrates that the RLBLOCA [

] However, the standard does not state a range of applicability of enrichment other than it is applicable to current operating LWRs. This section validates the [

]

A.2.1.1 Validation of Fission Product Decay Heat from 1979 and 2005 ANS Standards

Calculations are performed with the [] standards for the same conditions used with TRITON. The fission product decay heat values from each standard are compared to the TRITON values (generation of TRITON values are discussed in Section A.1) to ensure that the standards remain valid for enrichments up to [] U-235. The minimum, maximum, average, and standard deviation are presented in Table A-2 for the percent difference between each standard and the TRITON fission product decay heat results. [

] up to 62 GWd/MTU and shutdown times up to 10^6 seconds. Therefore, the standards remain valid for enrichments up to [] U-235.

Additionally, Section 8.5.1.17 of Reference 9 discusses RLBLOCA fission product decay heat predictions relative to low burnups and short decay times. Table A-2 shows that the results for [

]

A.2.1.2 RLBLOCA Fission Product Decay Heat Comparisons with ANS Standards

In Section 8.5.1.17 of Reference 9, the decay heat model for RLBLOCA is presented as [

]

Calculations are performed for []

U-235 fuel. []

] based on the results shown in

Figure A-1. To evaluate the impact of [] U-235 fuel, calculations using the same limiting conditions as in Reference 9 are repeated. The []

] As in

Section 8.5.1.17 of Reference 9, []

]

Figure A-4 and Figure A-5 []

]



A.2.2 RLBLOCA Actinide Decay Heat

The actinide decay heat model for RLBLOCA uses the actinide model in the 1979 Decay Heat Standard (Reference 29). [

As shown in Figure A-3, the actinide decay heat is [The 2014 ANS decay heat standard (Reference 30) states, “The contribution of the remaining actinides (other than ^{239}U and ^{239}Np), $P_{dA}(t, T)$, shall be specified and justified by the user.” Comparisons of the actinide decay heat calculations from TRITON [

]

[

These results are shown in Figure A-8 and Figure A-9 for [U-235, respectively. [

]

A.2.3 RLBLOCA Decay Heat Model Conclusions

In Sections A.2.1 and A.2.2 it is shown that the following aspects of decay heat remain applicable to fuel with enrichment up to [U-235.

- The ANS fission product decay heat standards are applicable for fuel up to [U-235
- [

]

- [

]

Therefore, [

] remains applicable to fuel with enrichment up to [U-235.

A.3 SBLOCA Decay Heat Model

The small break LOCA (SBLOCA) methodology (Reference 8) uses the Appendix K (App K) Decay Heat Model, which is the decay heat from Reference 31 plus a [

] The fission product decay heat model in Reference 31 [

] In Section A.2.1.2, the

RLBLOCA fission product decay heat model is shown to be applicable to fuel with up enrichment up to [] U-235. [

] A simple comparison of the SBLOCA fission product decay heat model to the RLBLOCA fission product decay heat model is shown in Table A-3. The SBLOCA fission product decay heat model is [] than the RLBLOCA model ranging between [] Therefore, the SBLOCA fission product decay heat model is applicable to fuel with enrichment up to [] U-235.

The [

] Therefore, the

total decay heat model (fission product plus actinide) for SBLOCA also remains applicable to fuel with enrichment up to [] U-235.

A.4 ARITA Decay Heat Models

ARITA (Reference 5) utilizes two decay heat models, one for the zero dimensional core model (labeled ARITA 0D) and the other is for the three dimensional core model (labeled ARITA coupled). The ARITA 0D model for fission product and actinide decay heat is identical to the RLBLOCA model and is therefore already validated for enrichments up to [] U-235. This section focuses on validation of the ARITA coupled decay heat model for enrichments greater than 5 wt% U-235.

The ARITA coupled method calculates a node by node decay heat for both fission products and actinides. The ARITA coupled fission product decay heat model uses

【] from the 2005 ANS
decay heat Standard (Reference 23). 【

】

The TRITON results for the total decay heat and fission product decay heat without uncertainties are used to validate the ARITA coupled decay heat model since 【

】 from ARITA coupled model is compared to the results compiled for TRITON in Section A.1. The comparisons for 【] U-235 are shown in Figure A-10 through Figure A-14 for various burnups. For 【

】 These results confirm that the ARITA coupled decay heat model 【] compared to a more robust best estimate method like TRITON. The decay heat model for the ARITA coupled methodology remains applicable for enrichments up to 【] U-235.

A.5 *Validity of Topical Report Decay Heat Models for Higher Enrichments*

Sections A.1 through A.4 provide a detailed evaluation of the impact of increasing enrichment up to [] U-235 upon the decay heat models used in the RLBLOCA, SBLOCA, and ARITA methodologies. The results show that the current decay heat model employed in each of these methodologies remains valid for use for fuel with enrichments up to [] U-235.

Table A-1
Topical Reports containing Decay Heat Methods

Topical Report	Fission Product Decay Heat Model	Actinide Decay Heat Model	TR Status
RLBLOCA (Reference 9)	[]	[]	Approved
SBLOCA (Reference 7)	Appendix K Decay Heat Model (Reference 31 +20%)	[]	Approved
ARITA (Reference 5)	ARITA 0D EM (Section 4.3.1 of Reference 29) -- Same as RLBLOCA.	[]	In Review
	ARITA Coupled EM (Section 5.1.2.1 and Section 9.1.1.15 of Reference 29) - []	[]	In Review

Table A-2
Comparison of Decay Heat Standards to TRITON results

Table A-3
Comparison of App K to RLBLOCA Results

Figure A-1
Total Decay Heat versus Burnup prior to Shutdown

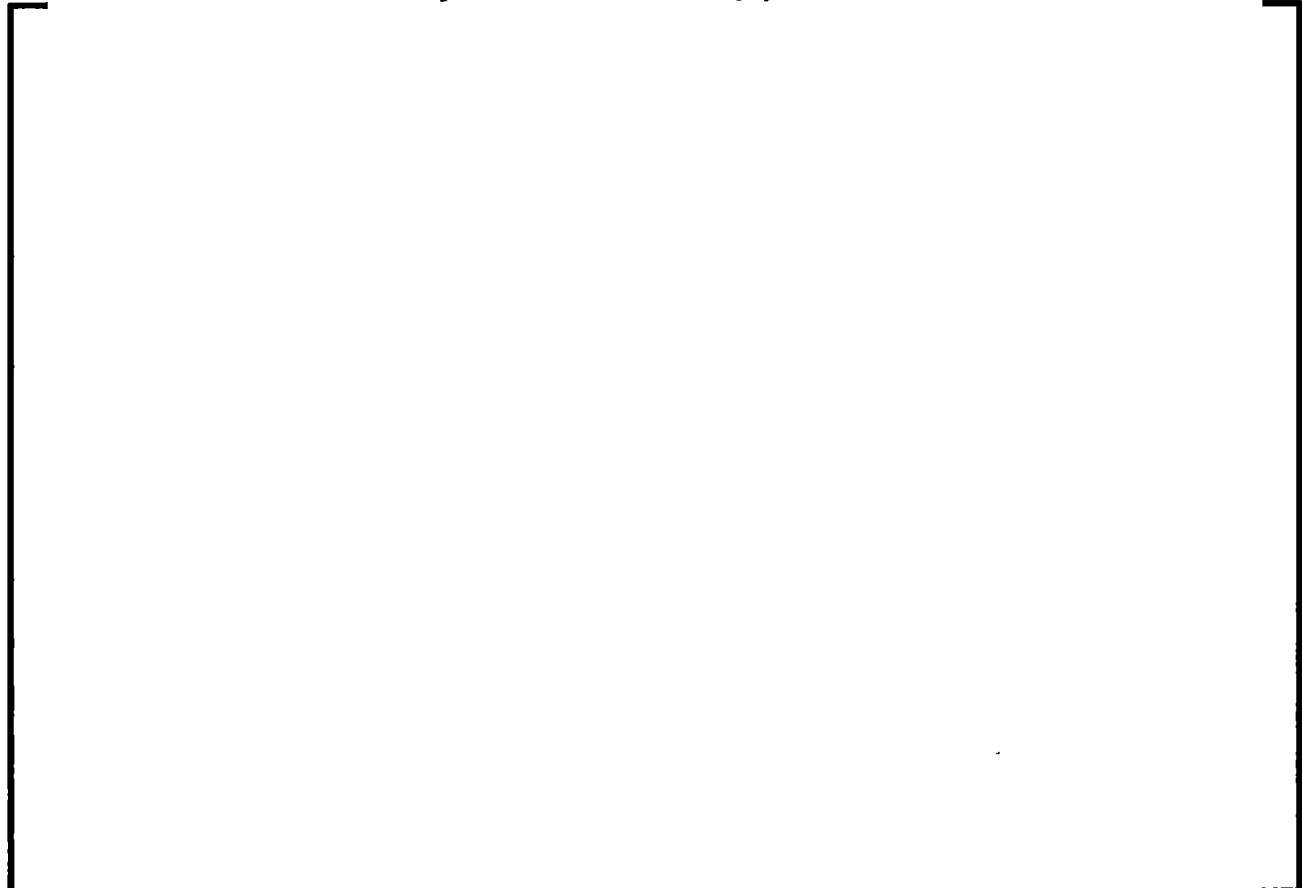


Figure A-2
Total Decay Heat versus Enrichment at []

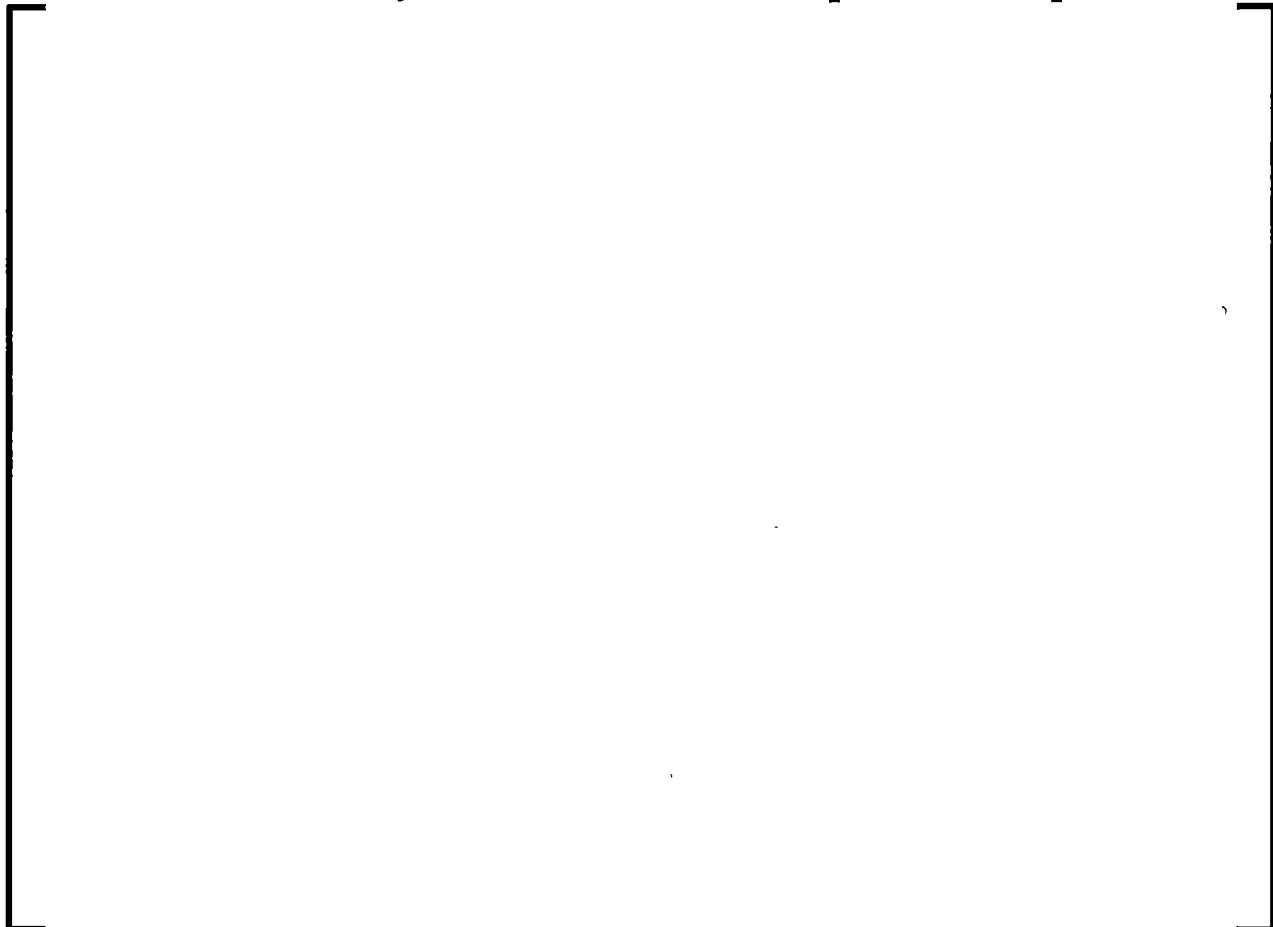


Figure A-3
Actinide Decay Heat versus Enrichment at []



Figure A-4
Decay Heat Comparisons, [
], All Isotopes

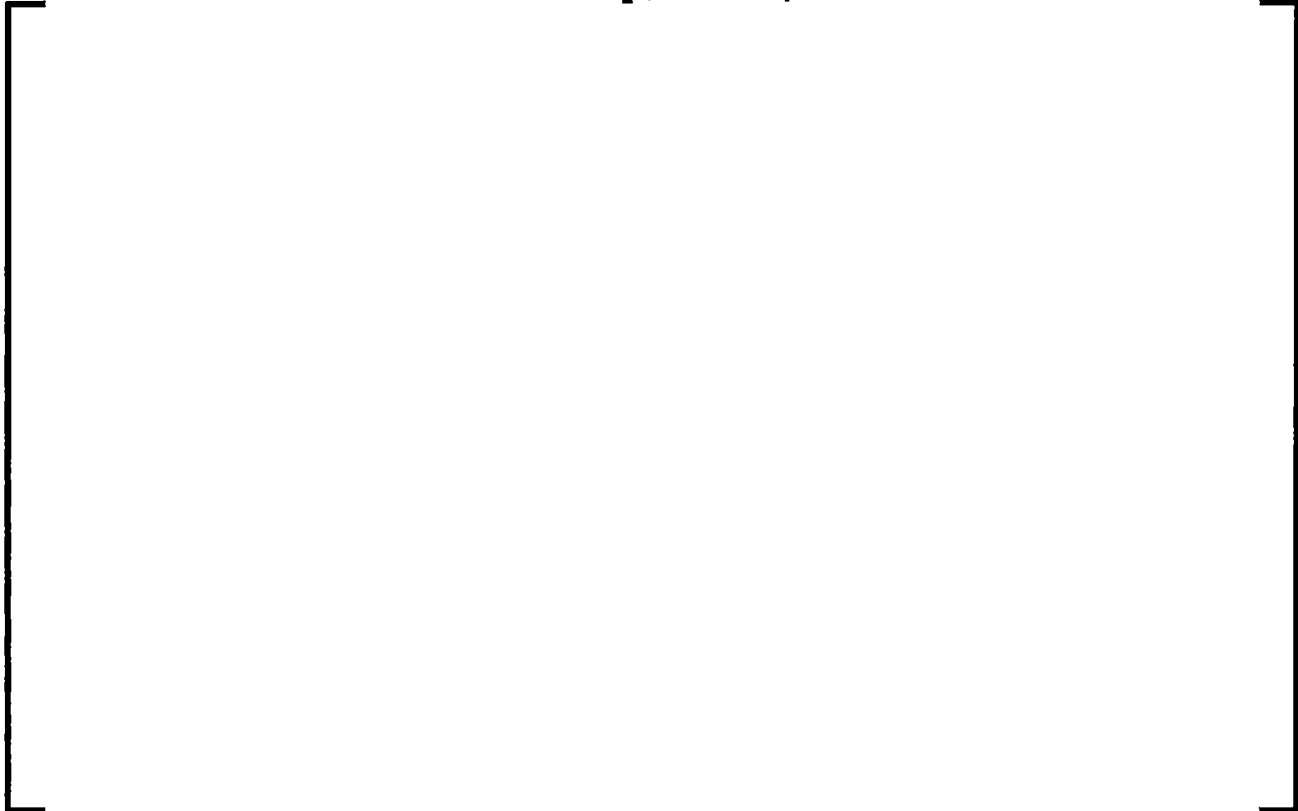


Figure A-5
Decay Heat Comparisons, [
Operation, All Isotopes **], Finite**



Figure A-6

Decay Heat Ratios, [

]

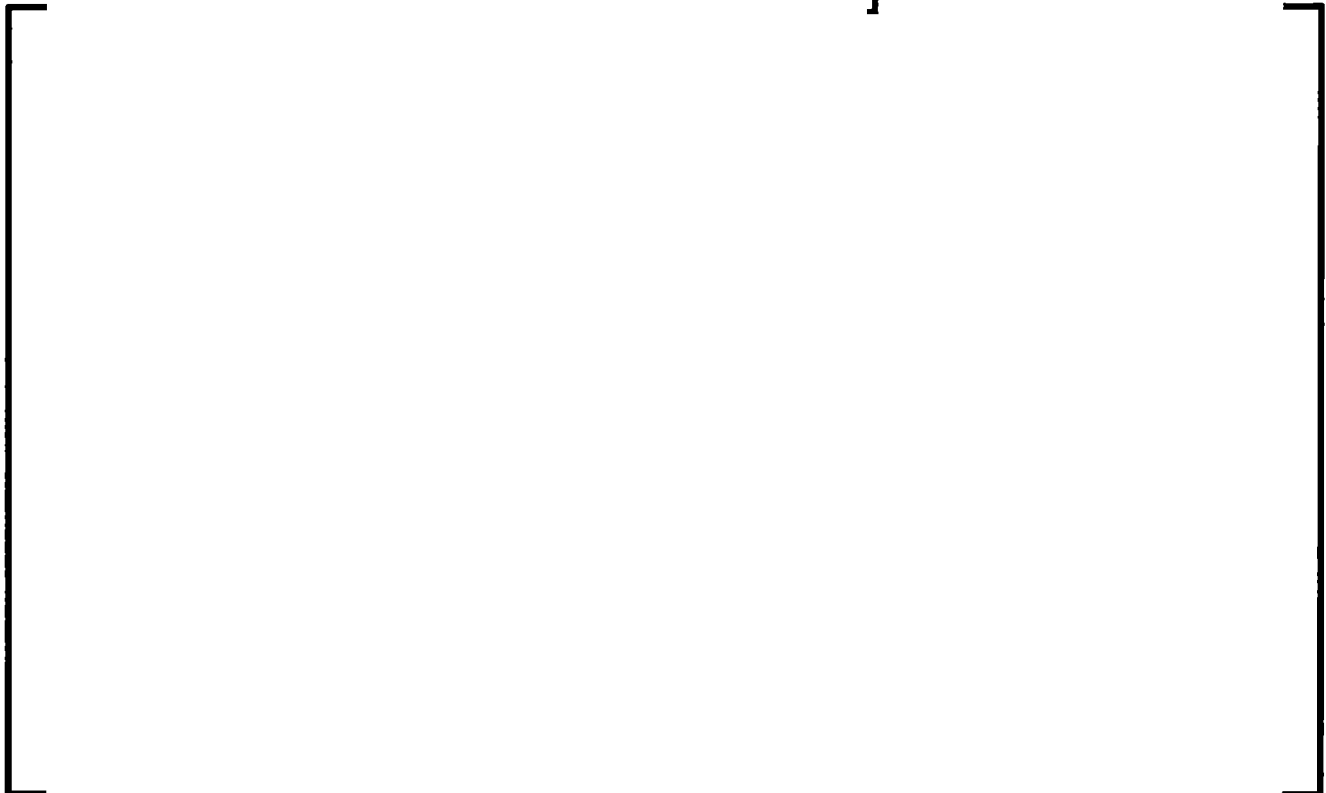


Figure A-7

Decay Heat Ratios, [

]



Figure A-8

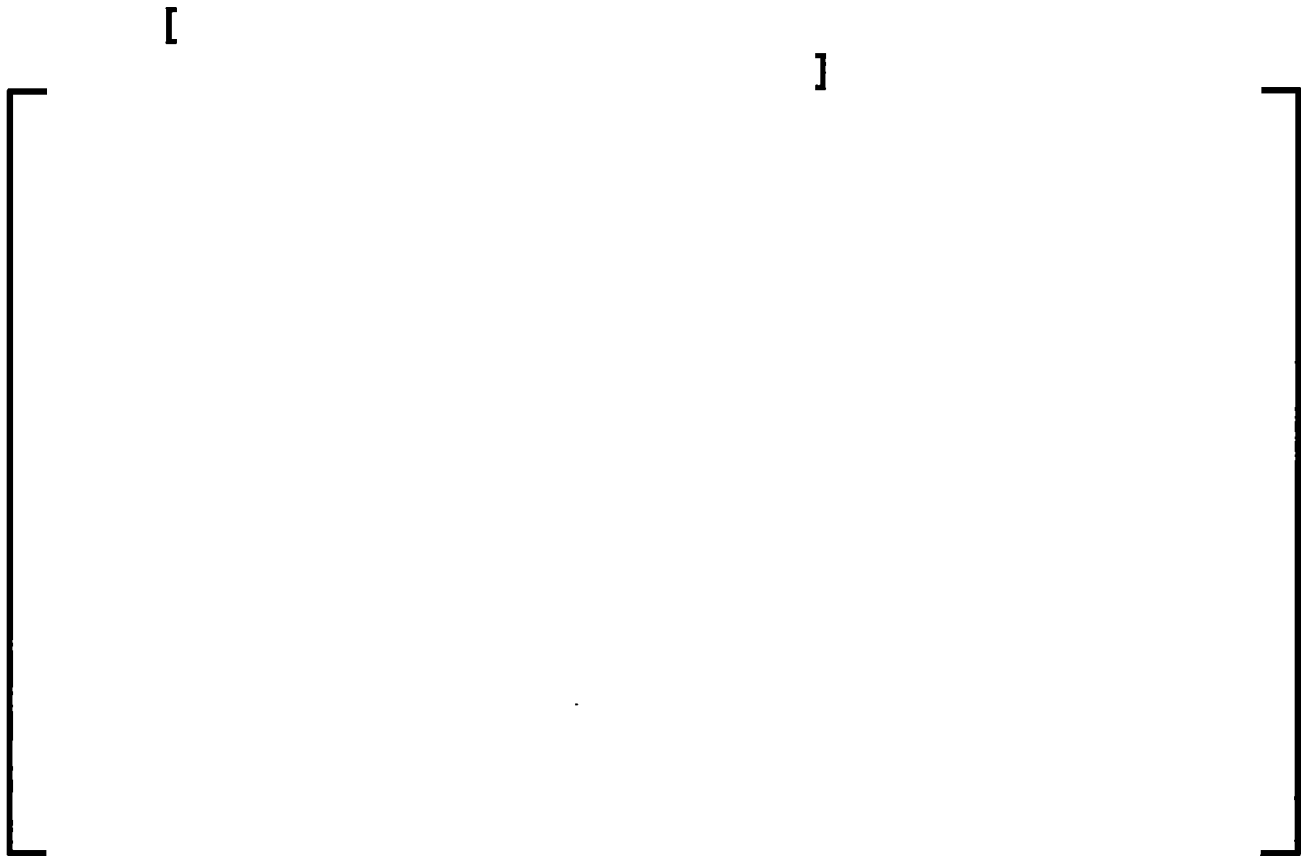


Figure A-9

[

]



Figure A-10
ARTEMIS versus TRITON Decay Heat at []



Figure A-11
ARTEMIS versus TRITON Decay Heat at []

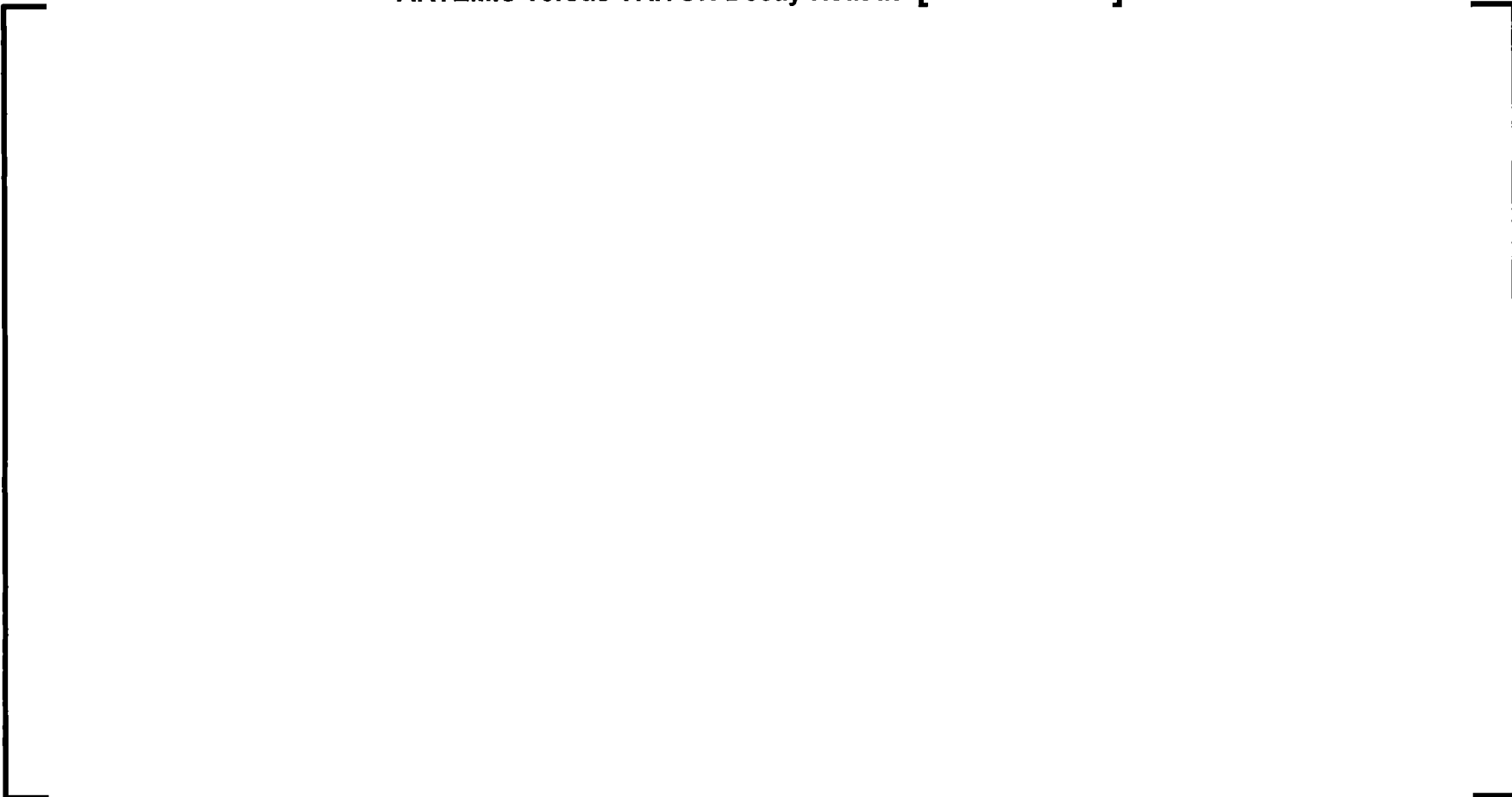


Figure A-12
ARTEMIS versus TRITON Decay Heat at []

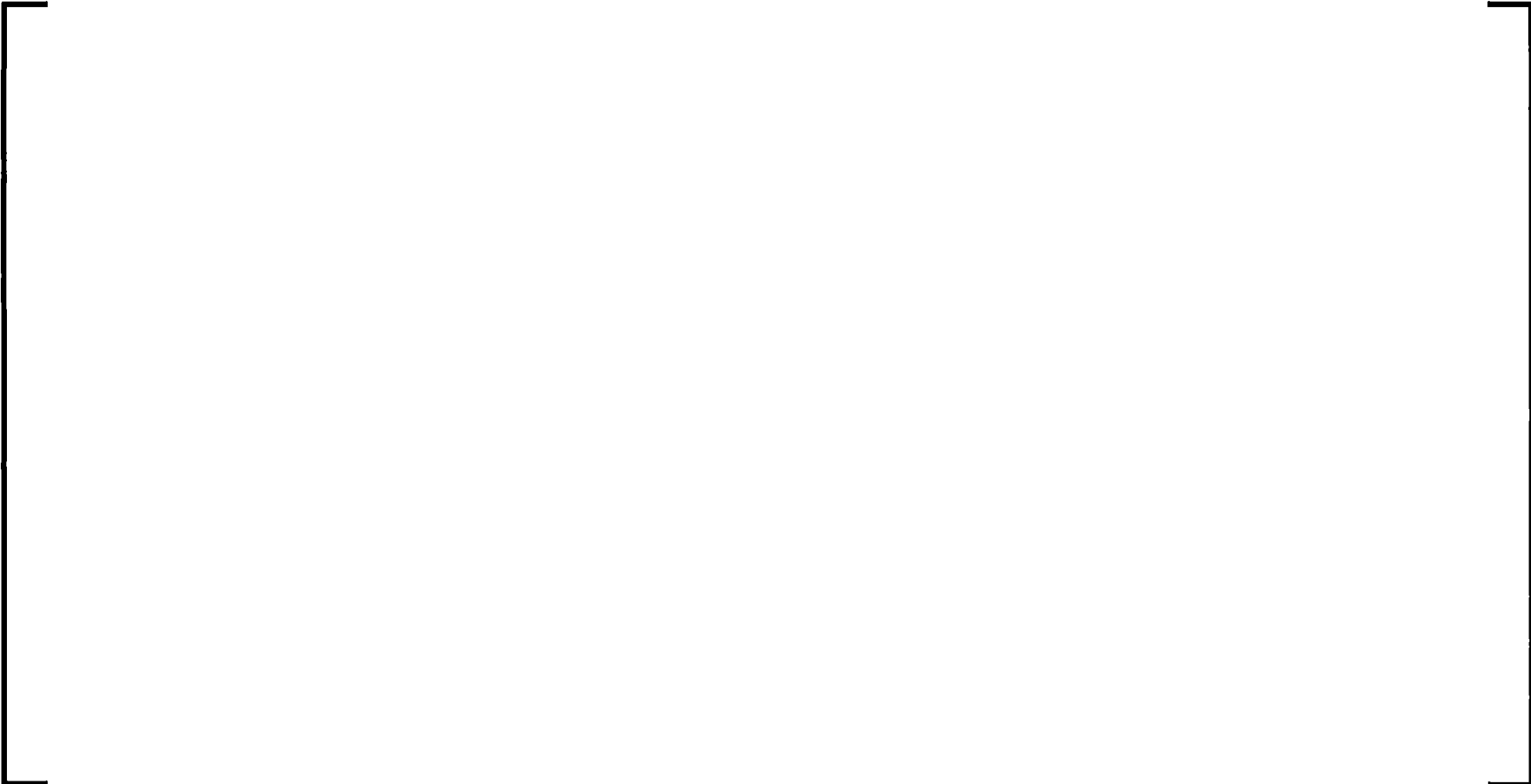


Figure A-13
ARTEMIS versus TRITON Decay Heat at []



Figure A-14
ARTEMIS versus TRITON Decay Heat at []

